Electronic Supplementary Information

Multicomponent covalent dye assembly for tight binding and sensitive sensing of L-DOPA

Xuan-Xuan Chen, Xin Wu, Peng Zhang, Miao Zhang, Bing-Nan Song, Yan-Jun Huang, Zhao Li, and Yun-Bao Jiang*

Department of Chemistry, College of Chemistry and Chemical Engineering, MOE Key Laboratory of Spectrochemical Analysis and Instrumentation, and Collaborative Innovation Center of Chemistry for Energy Materials (*i*ChEM), Xiamen University, Xiamen 361005, China

* E-mail: ybjiang@xmu.edu.cn

Contents

1. General

All commercial reagents and solvents were used as received. The synthesis of **1** has been reported previously.[1]

^{1}H NMR and ^{13}C NMR spectra were recorded on a Bruker AV500 NMR spectrometer. High-resolution mass spectra (HRMS) were taken on a Bruker En Apex ultra 7.0T FT-MS mass spectrometer. Absorption spectra were obtained on a Varian Cary 300 UV-Vis spectrophotometer, using a 1 cm quartz cuvette. Circular dichroism (CD) spectra were recorded on a Jasco J-810 CD spectropolarimeter, using a 1 cm quartz cuvette. Dynamic light scattering measurements were performed on a Malvern Zetasizer Nano ZS. Transmission electron microscope (TEM) images were taken on a JEOL JEM-1400 transmission electron microscope. All measurements were carried out at the ambient temperature of 298 K.

2. Synthesis and Characterization of Compounds 2-6

2.1 Synthesis

*Synthesis of **2***

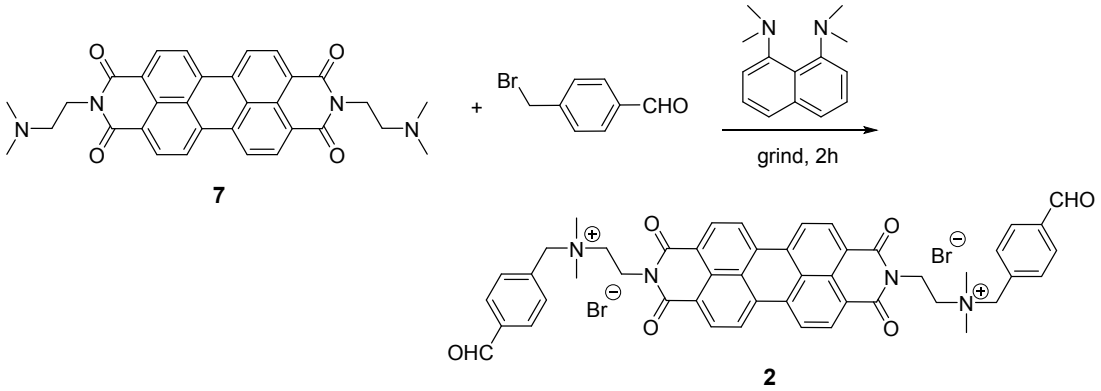

7

2

7[1] and 4-(bromomethyl)benzaldehyde[2] were synthesized according to reported procedures. **7** (0.11 g, 0.20 mmol), 4-(bromomethyl)benzaldehyde (0.10 g, 0.50 mmol), and 1,8-bis(dimethylamino)naphthalene (0.02 g, 0.1 mmol) was mixed and ground for 1 h, during which process several drops of MeCN was added to assist mixing. To the mixture was added 4-(bromomethyl)bezenzaldehyde (0.10 g, 0.50 mmol) and 1,8-bis(dimethylamino)naphthalene (0.02 g, 0.1 mmol) again, and the mixture was subject to further grinding for 1 h with several drops of MeCN. The residue was washed with MeOH and dried under vacuum to give **2** as a dark red solid (0.16 g, 86%).

^{1}H NMR (500 MHz, DMSO-d_6): δ (ppm) 10.12 (s, 2H), 8.90 (s, 4H), 8.57 (s, 4H), 8.07 (d, J = 8.2 Hz, 4H), 7.90 (d, J = 8.1 Hz, 4H), 4.86 (s, 4H), 4.63 (s, 4H), 3.68 (t, J = 6.5 Hz, 4H), 3.23 (s, 12H).

^{13}C NMR (126 MHz, CF_3COOD): δ (ppm) 196.60, 165.27, 137.23, 136.03, 133.76, 133.41, 133.08, 131.39, 129.22, 126.15, 124.41, 121.62, 68.81, 61.39, 50.13, 34.61.

HRMS (ESI-TOF) *m/z*: Calcd for $C_{48}H_{42}N_4O_6^{2+}$ 385.1552; Found 385.1539.

*Synthesis of **3***

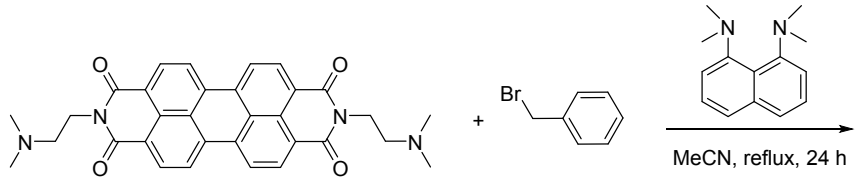

7

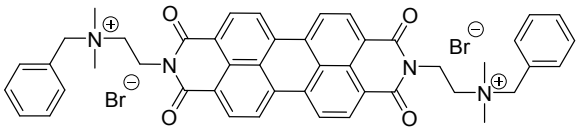

3

A mixture of **7** (0.11 g, 0.2 mmol), benzyl bromide (0.34 g, 4 mmol), and 1,8-bis(dimethylamino)naphthalene (0.17 g, 0.8 mmol) in MeCN was refluxed for 24 h. The solid was collected by filtration and heated under reflux in MeOH to completely remove benzyl bromide. The solid was collected by filtration and dried under vacuum to give **3** as a dark red solid (0.16 g, 92%).

^{1}H NMR (400 MHz, DMSO-d_6): δ (ppm) 8.96 (d, J = 8.0 Hz, 4H), 8.61 (d, J = 7.9 Hz, 4H), 7.68 – 7.62 (m, 4H), 7.58 – 7.51 (m, 6H), 4.73 (s, 4H), 4.61 (t, J = 7.4 Hz, 4H), 3.63 (t, J = 7.4 Hz, 4H), 3.17 (s, 12H).
^{13}C NMR (126 MHz, CF_3COOD): δ (ppm) 165.34, 136.04, 133.11, 132.48, 131.69, 129.54, 129.25, 126.17, 125.42, 124.44, 121.69, 70.21, 60.93, 49.71, 34.70.
HRMS (ESI-TOF) *m/z*: $[M]^{2+}$ Calcd for $C_{46}H_{42}N_4O_4^{2+}$ 357.1603; Found 357.1598.

*Synthesis of **4***

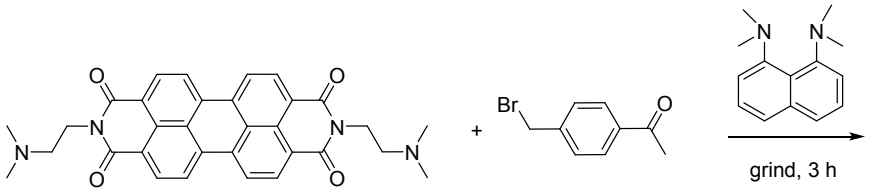

7

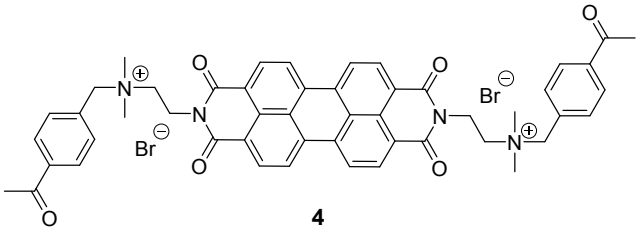

4

7 (0.10 g, 0.19 mmol), 1-(4-(bromomethyl)phenyl)ethanone (0.10 g, 0.47 mmol), and 1,8-bis(dimethylamino)naphthalene (0.10 g, 0.47 mmol) was mixed and ground for 3 h, during which process several drops of DMF was added to assist mixing. The residue was taken up in hot MeOH (50 mL) and the hot solution was filtered to remove insoluble **7**. The solution was concentrated to ~10 mL, to which Et_2O (50 mL) was added. A red precipitate was formed, which was subsequently collected by filtration, recrystallized again from MeOH-Et_2O and dried under vacuum (0.12 g, 65%).

^{1}H NMR (500 MHz, CF_3COOD): δ (ppm) 8.79 (s, 8H), 8.21 (d, J = 7.4 Hz, 4H), 7.79 (d, J = 7.3 Hz, 4H), 4.97 (s, 4H), 4.83 (s, 4H), 3.99 (s, 4H), 3.37 (s, 12H), 2.76 (s, 6H).
^{13}C NMR (126 MHz, CF_3COOD): δ (ppm) 204.61, 165.35, 138.24, 136.17, 133.28, 133.15, 131.85, 129.77, 129.27, 126.24, 124.42, 121.55, 68.83, 61.20, 50.04, 34.50, 24.83.
HRMS (ESI-TOF) *m/z*: $[M]^{2+}$ Calcd for $C_{50}H_{46}N_4O_6^{2+}$ 399.1703; Found 399.1701.

Synthesis of ***5***

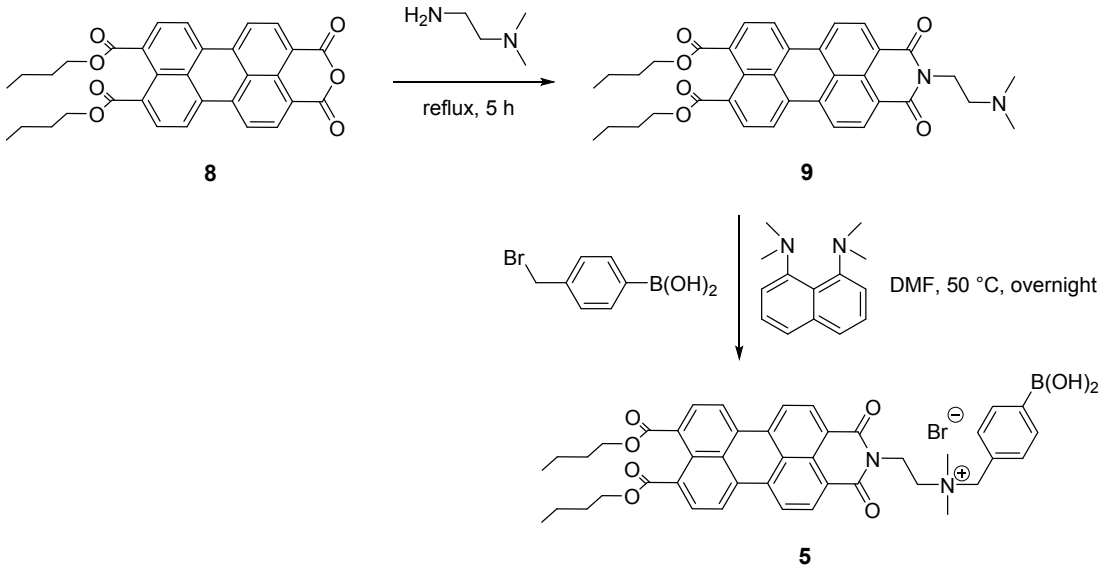

8 was synthesized following a literature procedure.[3] A suspension of **8** (0.27 g, 0.52 mmol) in *N*,*N*-dimethylethylenediamine (10 mL, 92 mmol) was refluxed for 5 h. After cooling, the reaction mixture was poured into Et_2O (50 mL). **9** precipitated as a dark red solid, and was separated by centrifugation, washed with Et_2O and dried under vacuum (0.29 g, 94%).

^{1}H NMR (500 MHz, DMSO-d_6): δ (ppm) 8.69 – 8.48 (m, 4H), 8.36 (s, 2H), 8.02 (d, J = 7.0 Hz, 2H), 4.27 (t, J = 6.7 Hz, 4H), 4.14 (t, J = 6.1 Hz, 2H), 2.24 (s, 6H), 1.84 – 1.62 (m, 4H), 1.52 – 1.38 (m, 4H), 0.96 (t, J = 7.4 Hz, 6H).

A mixture of **9** (0.10 g, 0.17 mmol), 4-(bromomethyl)phenylboronic acid (0.10 g 0.47 mmol), and 1,8-bis(dimethylamino)naphthalene (0.10 g, 0.47 mmol) was suspended in DMF (10 mL) and stirred at 50 °C overnight. After the reaction mixture cooled to room temperature, Et_2O (50 mL) was added. A red precipitate was formed, which was collected by filtration, washed several times with MeOH-Et_2O (2:1) and dried under vacuum (0.13 g, 95%).

^{1}H NMR (500 MHz, DMSO-d_6): δ (ppm) 8.84 – 8.73 (m, 4H), 8.50 (d, J = 8.0 Hz, 2H), 8.23 (s, 2H), 8.11 (d, J = 7.9 Hz, 2H), 7.92 (d, J = 7.8 Hz, 2H), 7.60 (d, J = 7.9 Hz, 2H), 4.70 (s, 2H), 4.53 (t, J = 7.0 Hz, 2H), 4.28 (t, J = 6.7 Hz, 4H), 3.57 (t, J = 7.0 Hz, 2H), 3.15 (s, 6H), 1.77 – 1.67 (m, 4H), 1.49 – 1.39 (m, 4H), 0.95 (t, J = 7.4 Hz, 6H).

^{13}C NMR (126 MHz, DMSO-d_6): δ (ppm) 167.59, 162.76, 135.02, 134.52, 132.08, 131.62, 131.33, 131.16, 130.41, 129.26, 128.54, 128.17, 128.07, 125.17, 123.90, 122.86, 121.45, 67.02, 65.09, 59.76, 49.38, 33.44, 30.08, 18.73, 13.66.
HRMS (ESI-TOF) *m/z*: $[M + 2CH_3OH - 2H_2O]^+$ Calcd for $C_{45}H_{48}BN_2O_8^+$ 755.3504; Found 755.3509.

Synthesis of ***6***

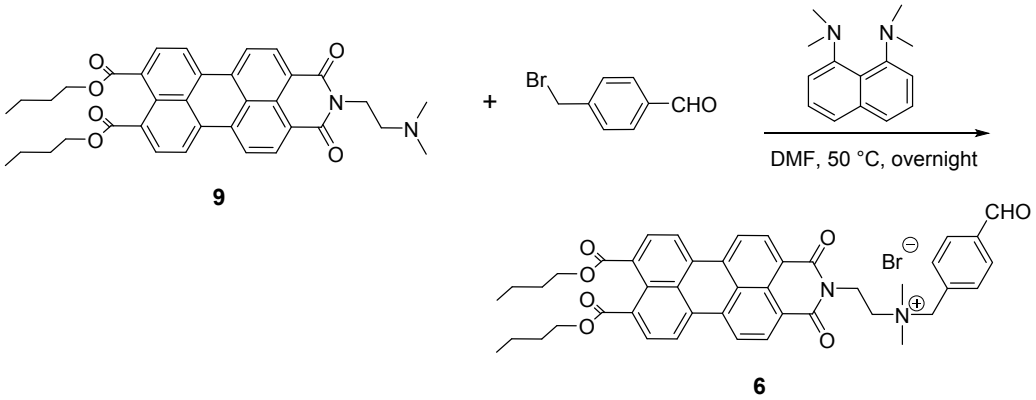

9 **6**

A mixture of **9** (0.10 g, 0.17 mmol), 4-(bromomethyl)benzaldehyde (0.10 g, 0.50 mmol), and 1,8-bis(dimethylamino)naphthalene (0.10 g, 0.47 mmol) was suspended in DMF (10 mL) and stirred at 50 °C overnight. After the reaction mixture cooled to room temperature, Et_2O (50 mL) was added. A red precipitate was formed, which was collected by filtration, washed several times with Et_2O and dried under vacuum (0.13 g, 98%).

^{1}H NMR (500 MHz, DMSO-d_6): δ (ppm) 10.11 (s, 1H), 8.87 – 8.67 (m, 4H), 8.48 (d, J = 7.6 Hz, 2H), 8.10 (d, J = 7.8 Hz, 2H), 8.06 (d, J = 7.9 Hz, 2H), 7.87 (d, J = 7.9 Hz, 2H), 4.82 (s, 2H), 4.53 (t, J = 7.0 Hz, 2H), 4.28 (t, J = 6.6 Hz, 4H), 3.60 (t, J = 7.0 Hz, 2H), 3.19 (s, 6H), 1.77 – 1.67 (m, 4H), 1.50 – 1.36 (m, 4H), 0.95 (t, J = 7.4 Hz, 6H).
^{13}C NMR (126 MHz, DMSO-d_6): δ (ppm) 193.04, 167.58, 162.85, 137.24, 135.11, 133.97, 133.81, 131.67, 131.37, 131.22, 130.44, 129.77, 128.63, 128.23, 128.11, 125.27, 123.95, 122.93, 121.54, 66.29, 65.10, 60.21, 49.56, 33.46, 30.08, 18.73, 13.67.
HRMS (ESI-TOF) *m/z*: $[M]^+$ Calcd for $C_{44}H_{43}N_2O_7^+$ 711.3065; Found 711.3053.

2.2 NMR spectra

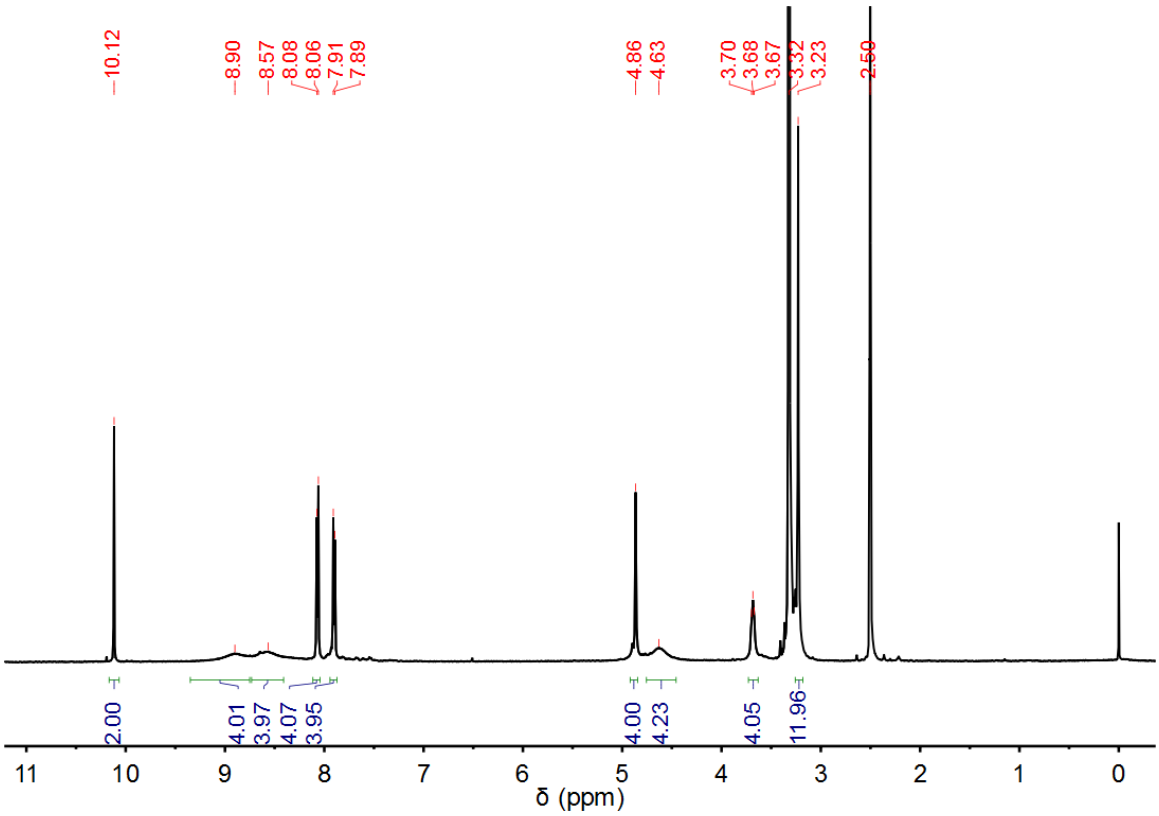

Fig. S1 ^{1}H NMR spectrum (500 MHz) of **2** in DMSO-d_6.

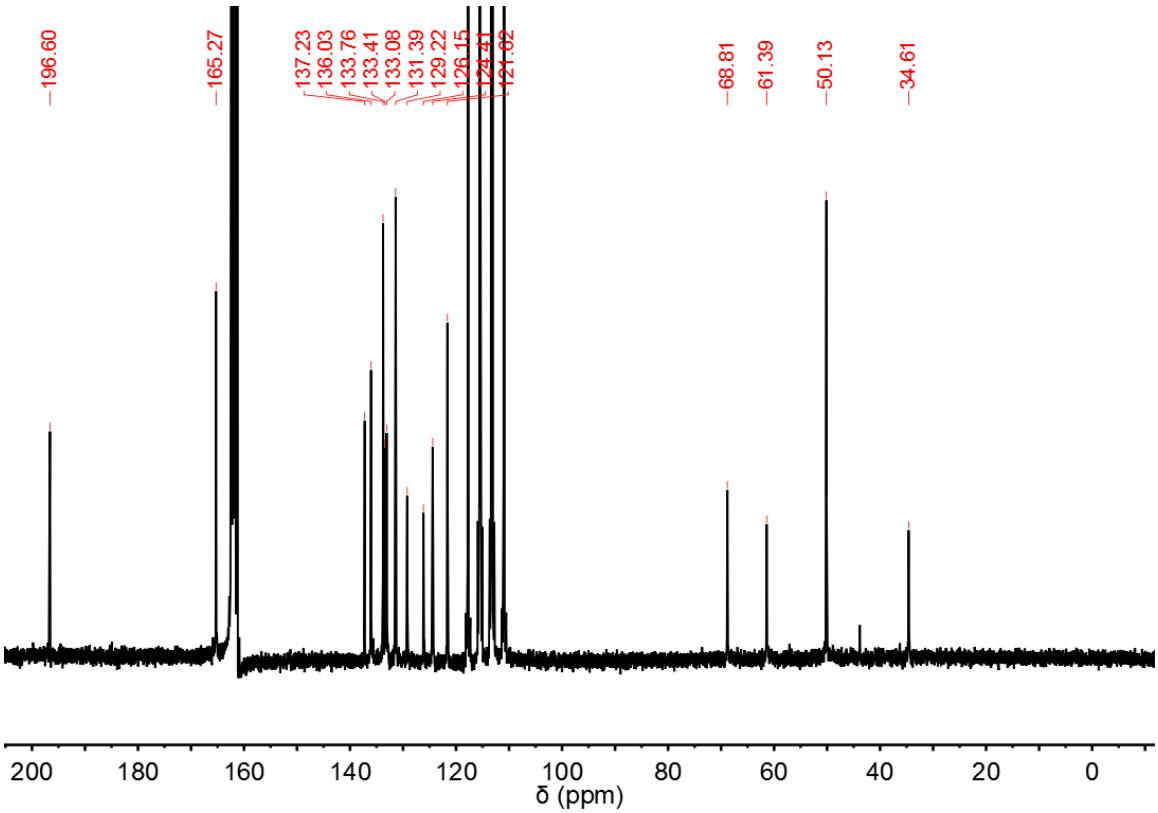

Fig. S2 ^{13}C NMR spectrum (126 MHz) of **2** in CF_3COOD.

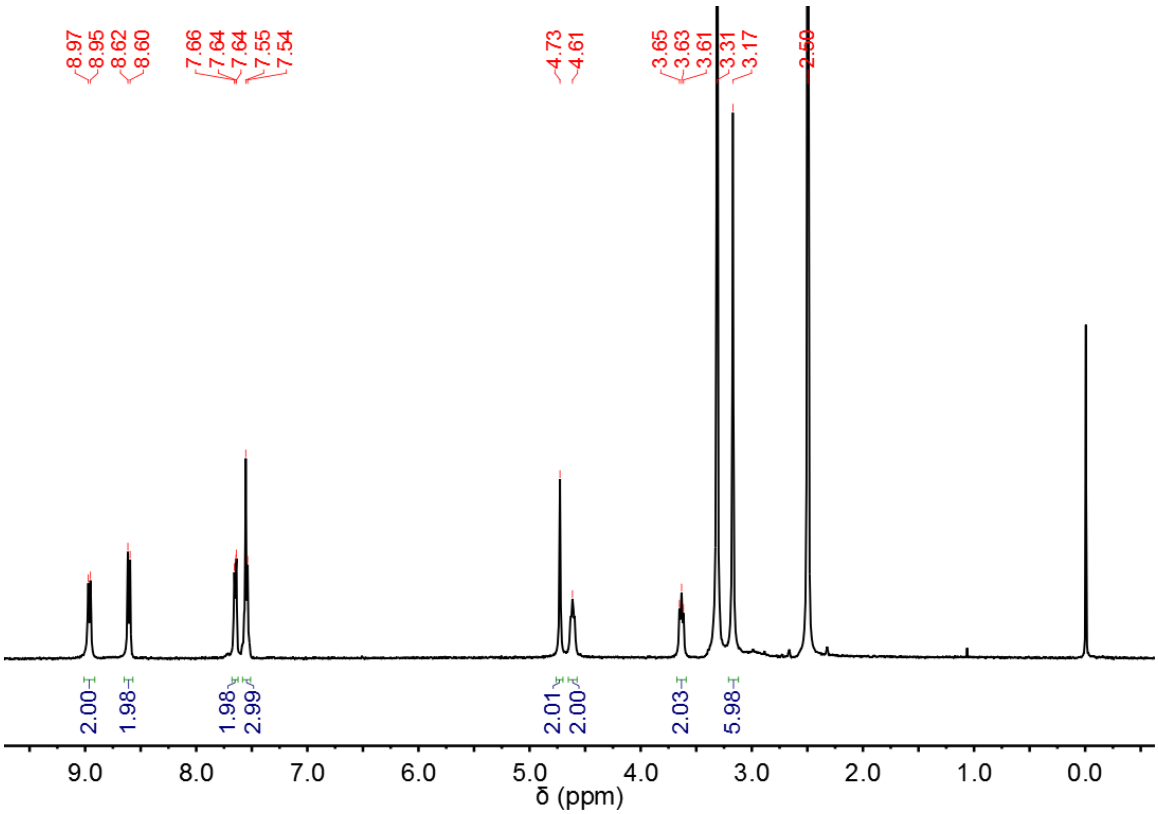

Fig. S3 ^{1}H NMR spectrum (400 MHz) of **3** in DMSO-d_6.

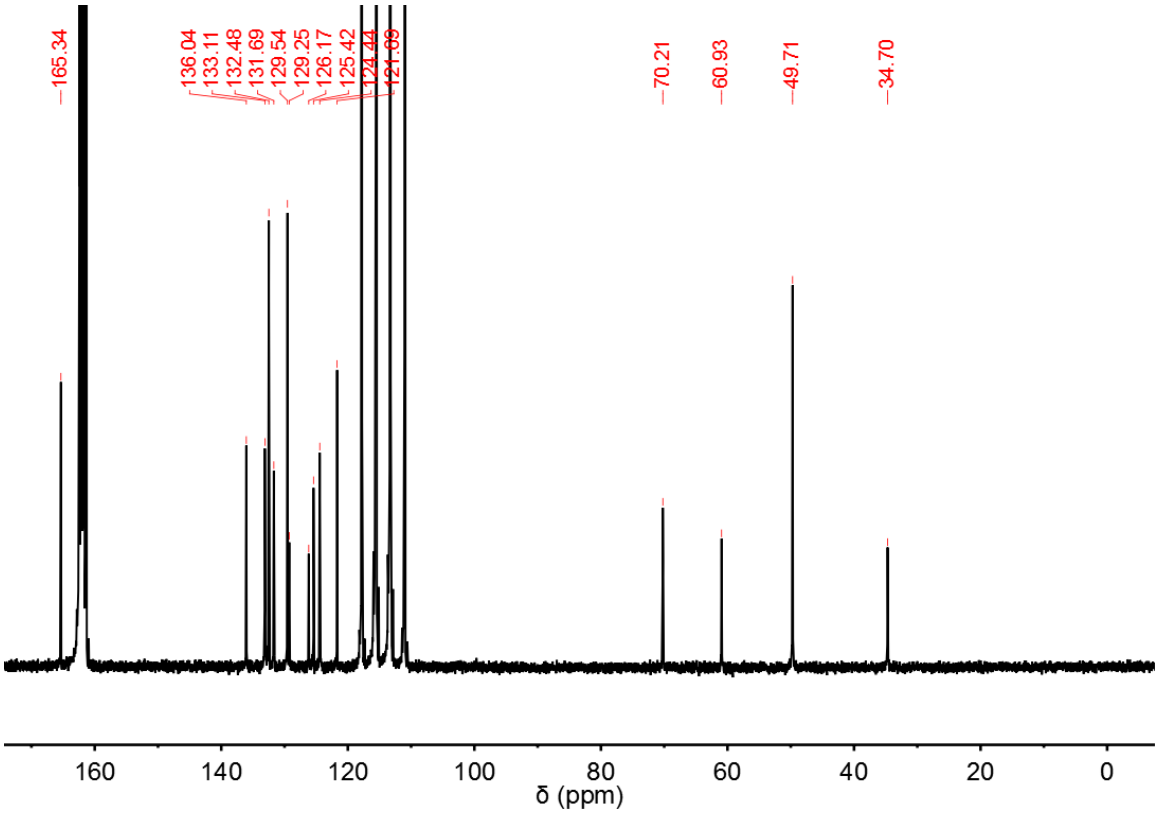

Fig. S4 ^{13}C NMR spectrum (126 MHz) of **3** in CF_3COOD.

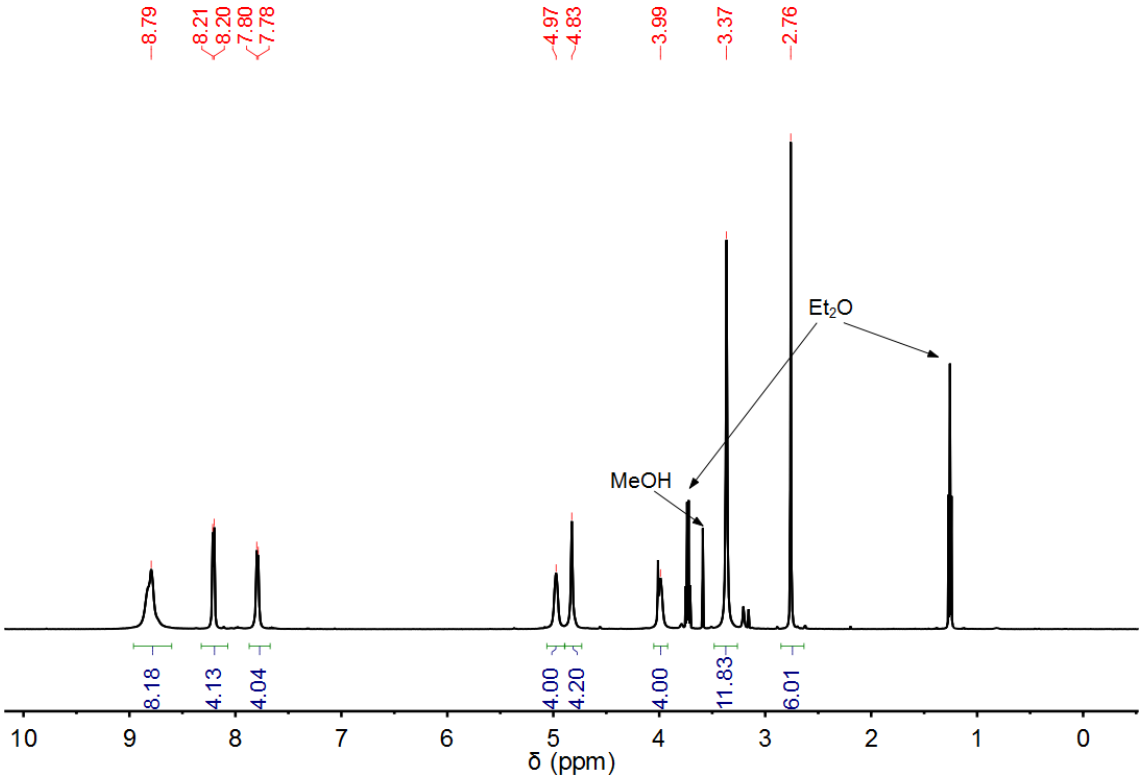

Fig. S5 ^{1}H NMR spectrum (500 MHz) of **4** in CF_3COOD.

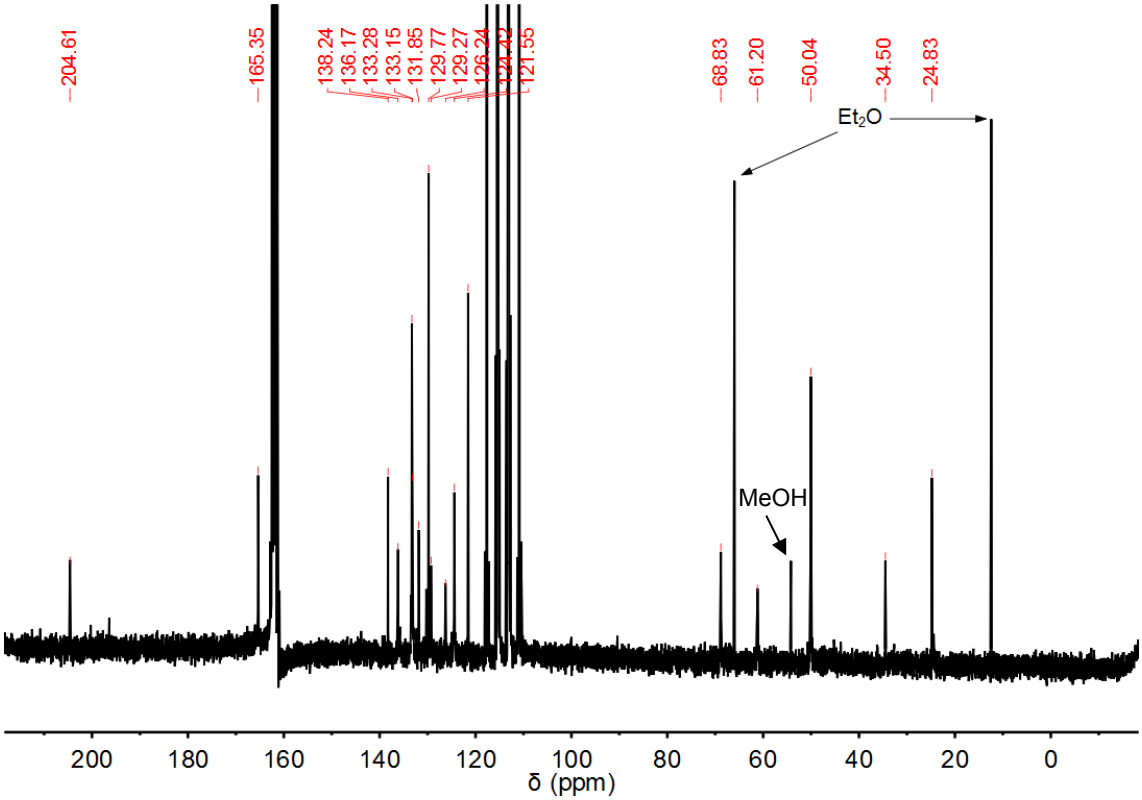

Fig. S6 ^{13}C NMR spectrum (126 MHz) of **4** in CF_3COOD.

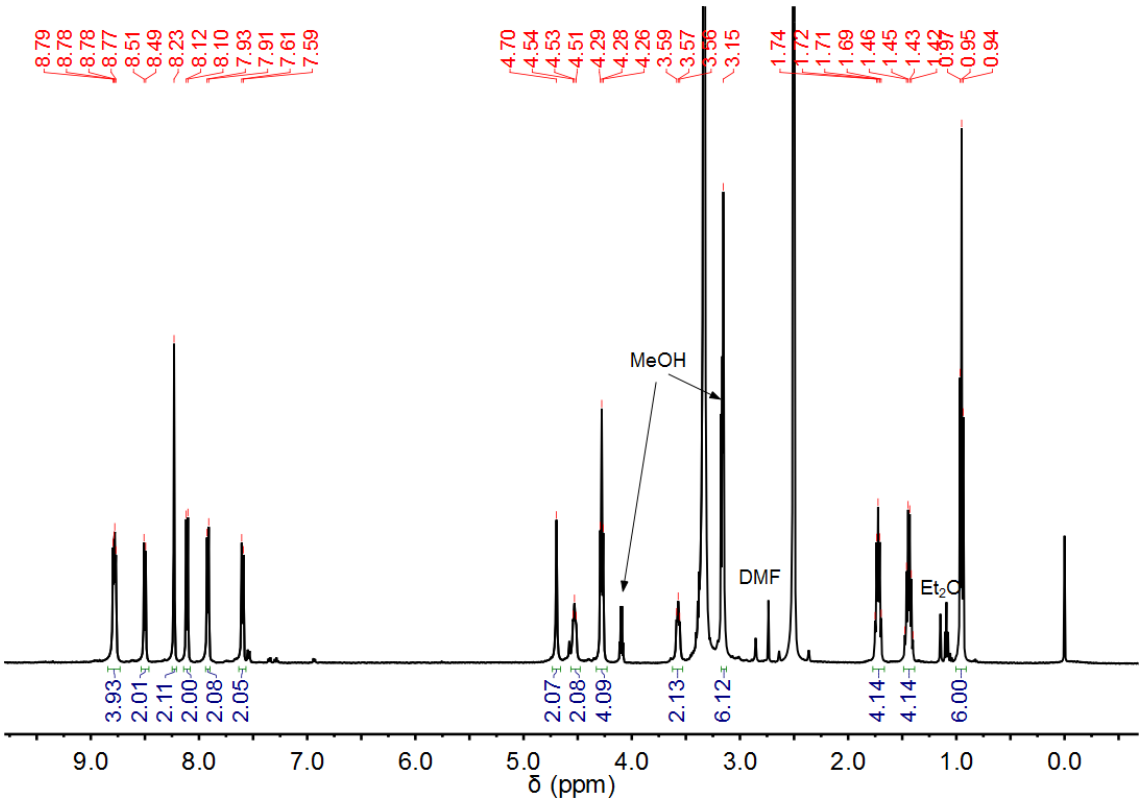

Fig. S7 ^{1}H NMR spectrum (500 MHz) of **5** in DMSO-d_6.

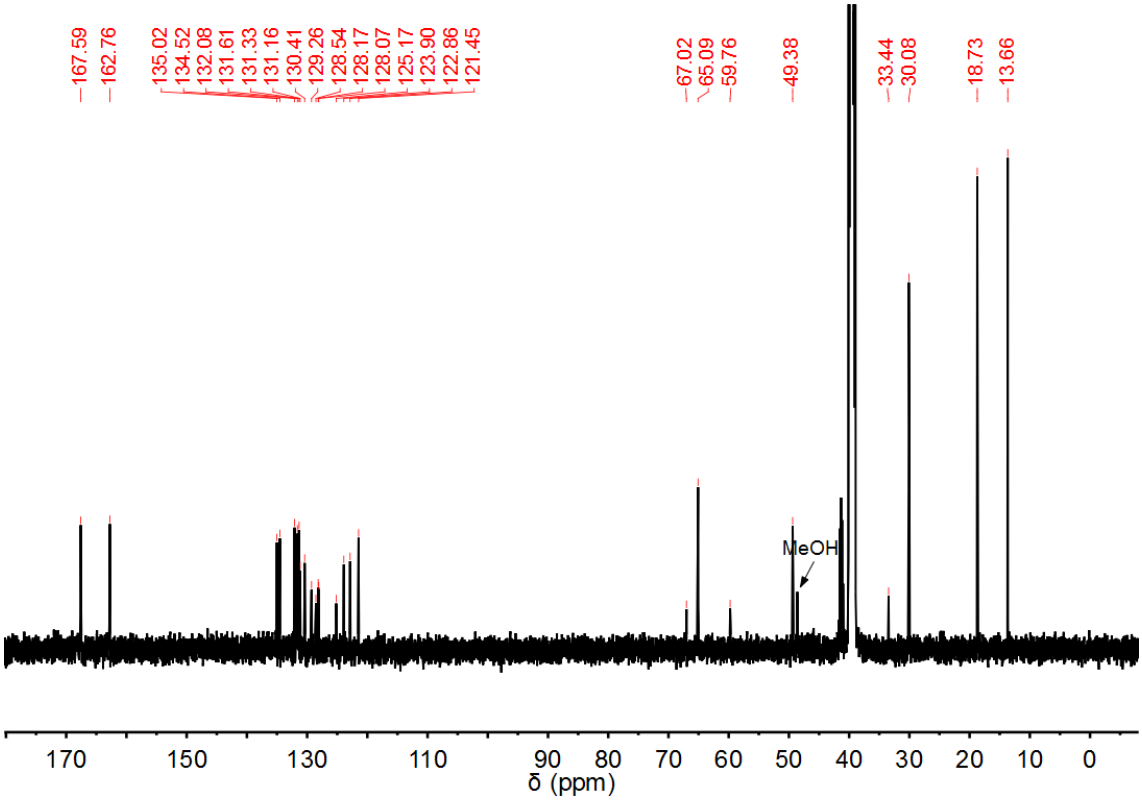

Fig. S8 ^{13}C NMR spectrum (126 MHz) of **5** in DMSO-d_6.

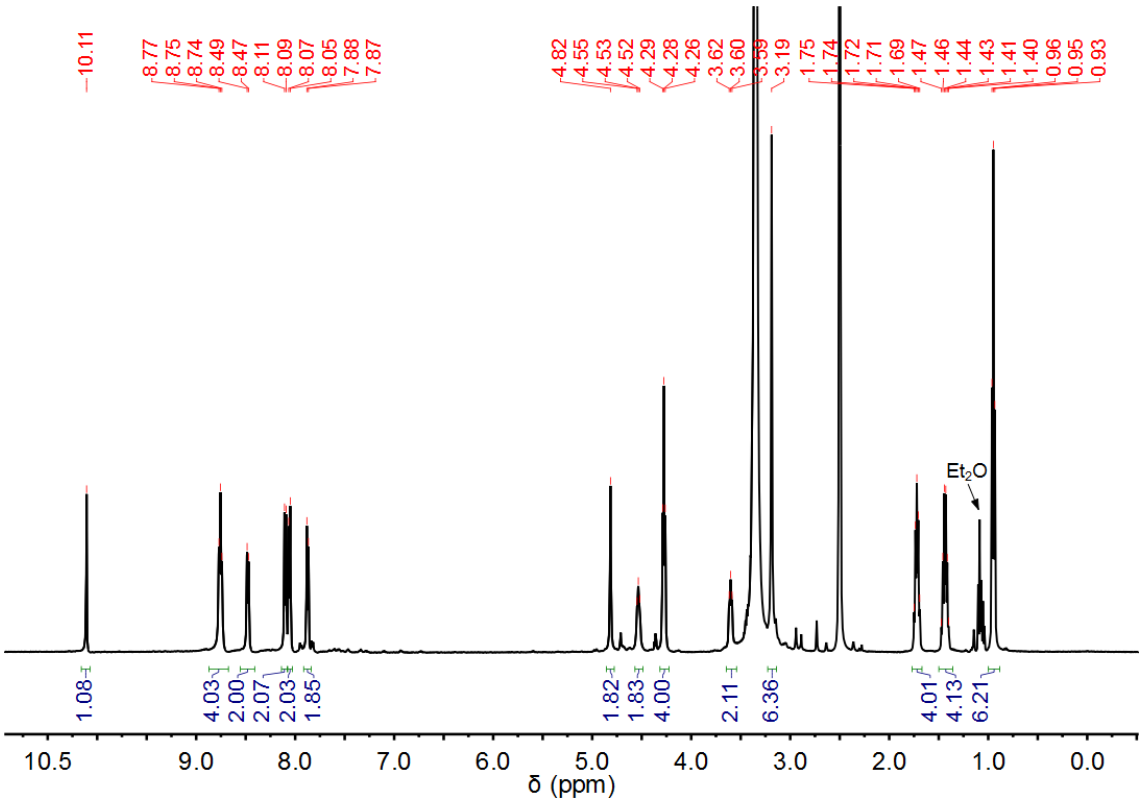

Fig. S9 ^{1}H NMR spectrum (500 MHz) of **6** in DMSO-d_6.

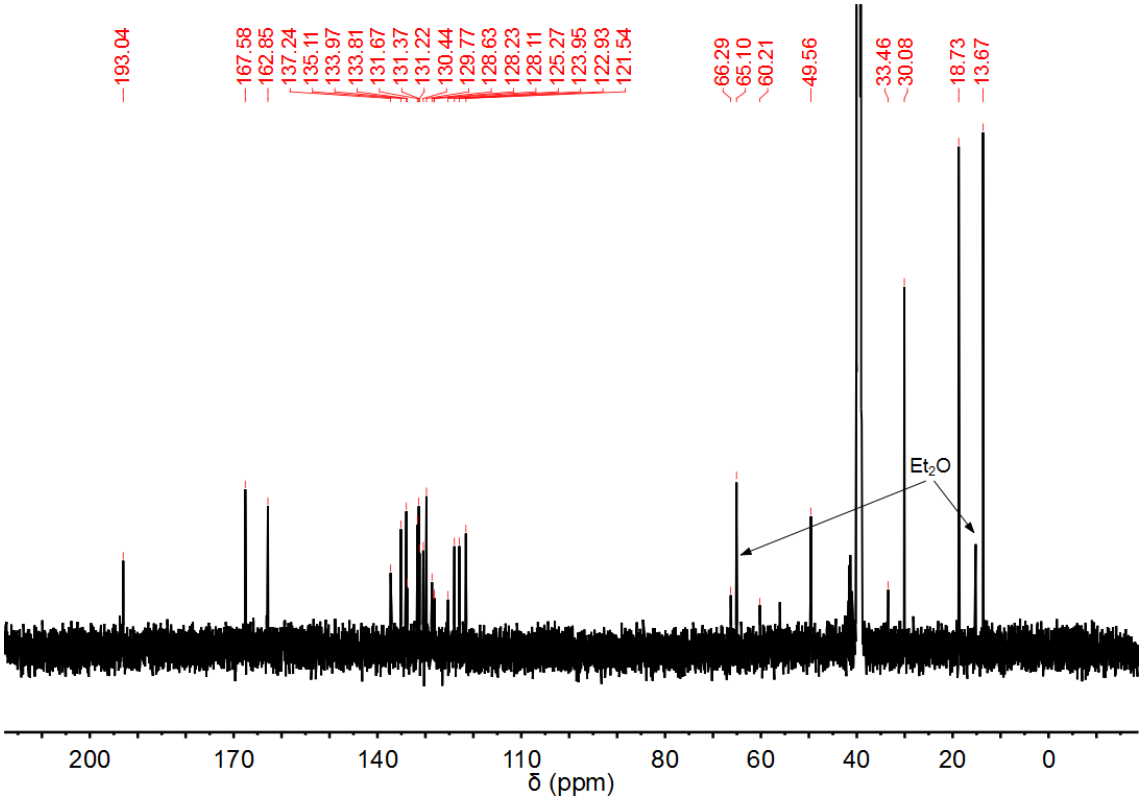

Fig. S10 ^{13}C NMR spectrum (126 MHz) of **6** in DMSO-d_6.

3. Sample Preparation

Stock solutions of perylene dyes **1** (2 mM), **5** (2 mM) and **6** (2 mM) were prepared in MeOH. Stock solutions of perylene dyes **2** (2 mM), **3** (2 mM) and **4** (2 mM) were prepared in DMSO. The buffer solution used was 50 mM HEPES-NaOH at pH 7.5. To 2.0 mL aqueous buffer solution containing the desired concentration of L-DOPA or other guests was added the stock solutions of PBI dyes to the desired host concentration. In the cases of mixed dyes, stock solution of the non-boronic acid dye component (**2**, **3**, **4** or **6**) was added to the aqueous solutions prior to the addition of stock solution of the boronic acid-functionalised dye (**1** or **5**)**.** The resultant solutions were allowed to stand for 1 h before being subject to spectroscopic or DLS measurements. For TEM images, the solutions prepared as stated above were pipetted onto a copper grid, dried under vacuum for 1 h before TEM imaging.

4. Data Analysis

Apparent binding constants (K) for 1:1 stoichiometry were calculated by fitting the UV-Vis absorption titration data to eq 1, where c is the host concentration, x is the guest concentration, y_0 is the signal at zero guest concentration, y_m is the signal at infinite guest concentration, K is the binding constant.

$$y = y_0 + \frac{y_m - y_0}{2c}(c + x + 1/K - \sqrt{(c + x + 1/K)^2 - 4cx}) \quad (1)$$

In general, the absorbance at 501 nm decreases with increasing guest concentration due to enhanced aggregation of PBI-based receptors. When reversal of this trend was observed with high guest concentrations, presumably due to guest binding beyond the initial 2 : 1 (host to guest) stoichiometry, the high concentration data points were excluded from the curve fitting. The values should therefore be regarded as relative values for comparison among different systems.

5. Spectroscopic Binding Studies

5.1 Compounds 1 and 2 and their mixture

5.1.1 UV-Vis absorption spectra

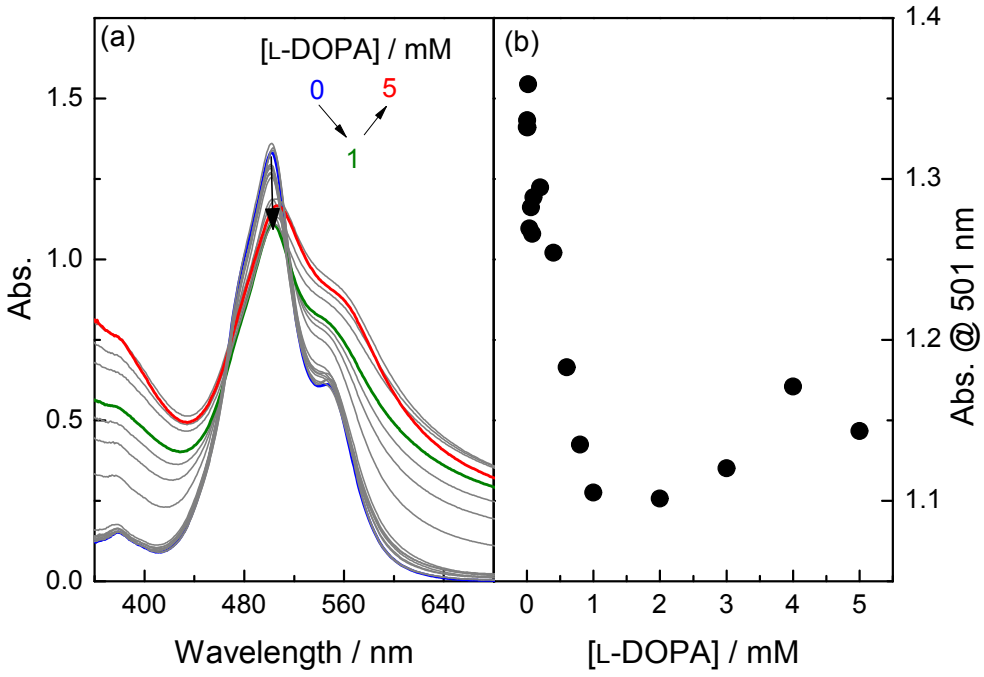

Fig. S11 (a) Absorption spectra of **1** (50 μM) with increasing concentration of L-DOPA in pH 7.5 HEPES buffer. (b) Absorbance of **1** at 501 nm vs concentration of L-DOPA.

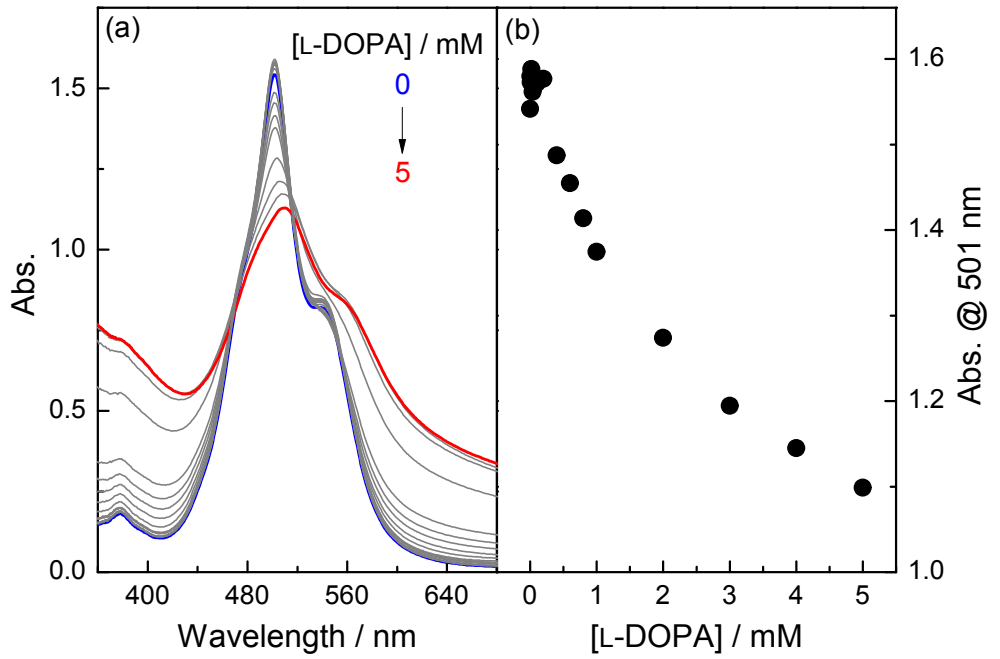

Fig. S12 (a) Absorption spectra of **2** (50 μM) with increasing concentration of L-DOPA in pH 7.5 HEPES buffer. (b) Absorbance of **2** at 501 nm vs concentration of L-DOPA.

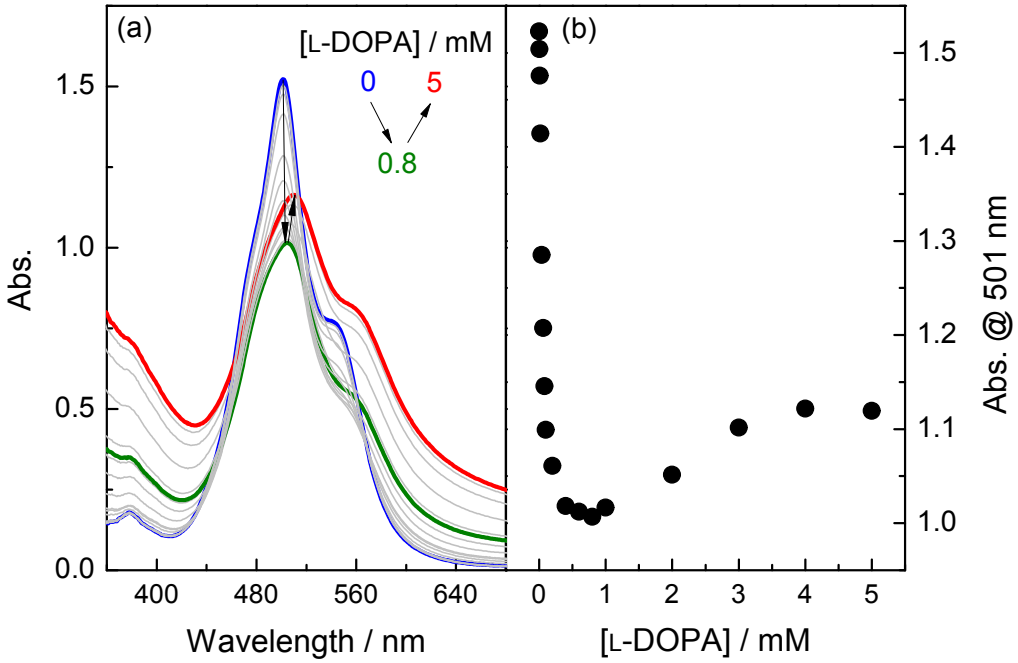

Fig. S13 (a) Absorption spectra of a mixture of **1** (25 μM) and **2** (25 μM) with increasing concentration of L-DOPA in pH 7.5 HEPES buffer. (b) Absorbance of a mixture of **1** and **2** at 501 nm vs concentration of L-DOPA.

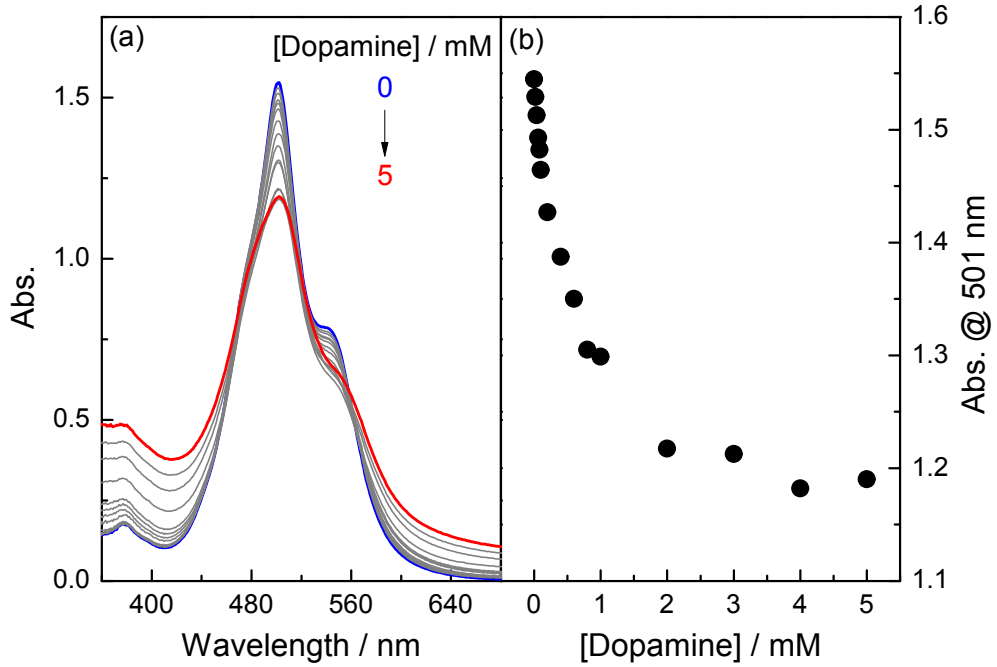

Fig. S14 (a) Absorption spectra of a mixture of **1** (25 μM) and **2** (25 μM) with increasing concentration of dopamine in pH 7.5 HEPES buffer. (b) Absorbance of a mixture of **1** and **2** at 501 nm vs concentration of dopamine.

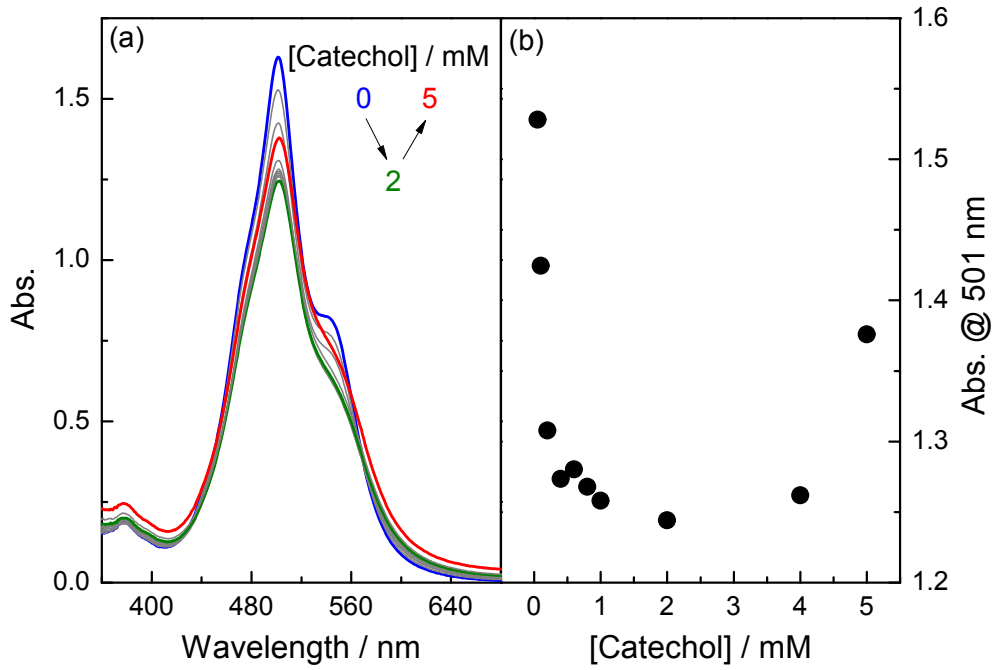

Fig. S15 (a) Absorption spectra of a mixture of **1** (25 μM) and **2** (25 μM) with increasing concentration of catechol in pH 7.5 HEPES buffer. (b) Absorbance of a mixture of **1** and **2** at 501 nm vs concentration of catechol.

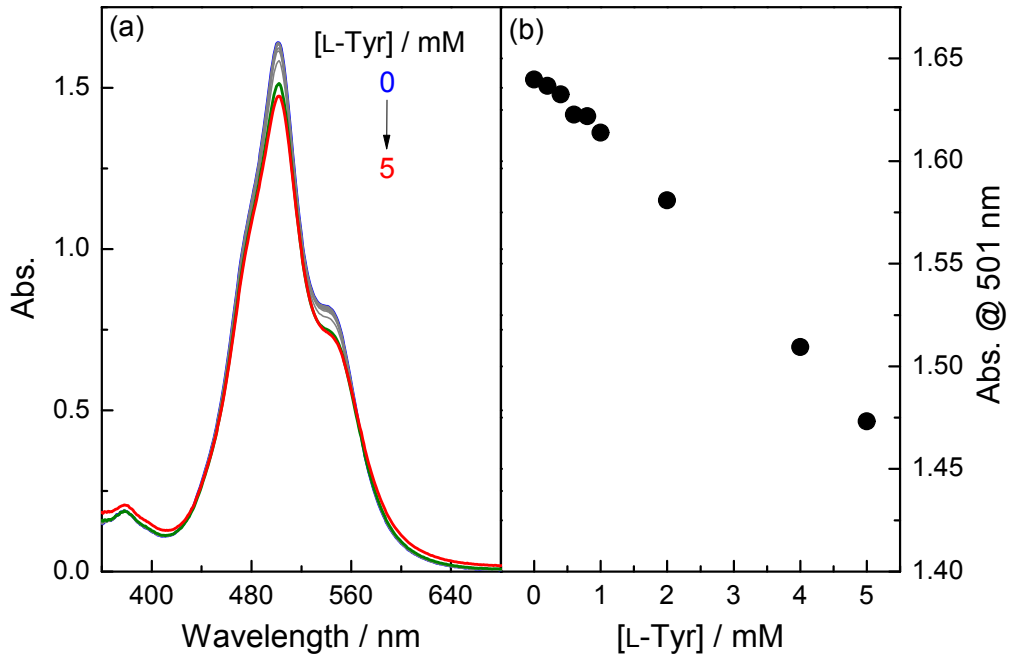

Fig. S16 (a) Absorption spectra of a mixture of **1** (25 μM) and **2** (25 μM) with increasing concentration of L-Tyr in pH 7.5 HEPES buffer. (b) Absorbance of a mixture of **1** and **2** at 501 nm vs concentration of L-Tyr.

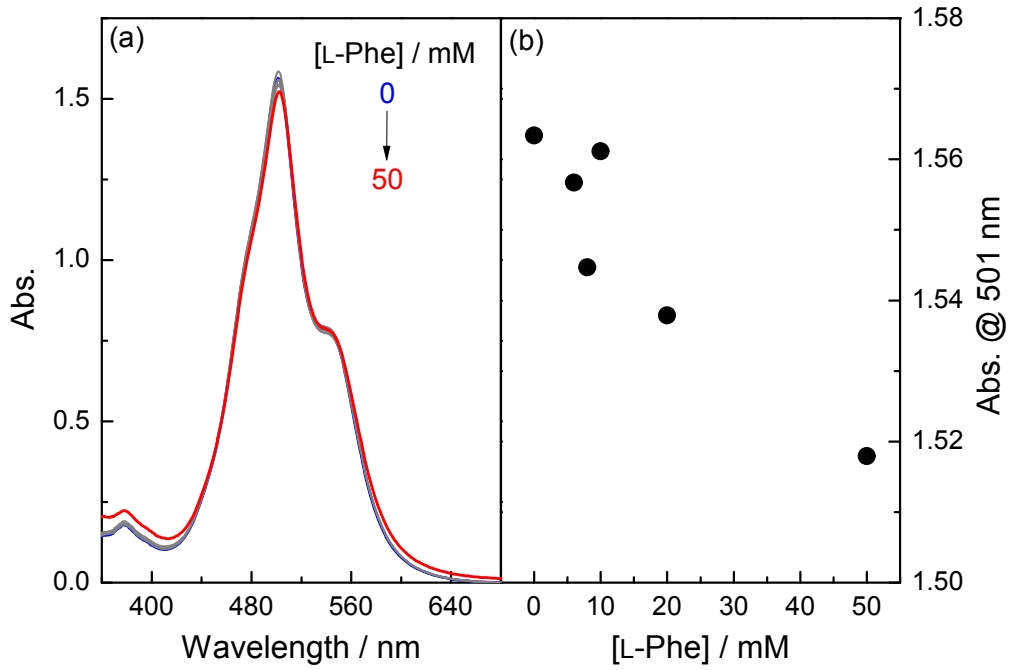

Fig. S17 (a) Absorption spectra of a mixture of **1** (25 μM) and **2** (25 μM) with increasing concentration of L-Phe in pH 7.5 HEPES buffer. (b) Absorbance of a mixture of **1** and **2** at 501 nm vs concentration of L-Phe.

5.1.2 Binding constant determination

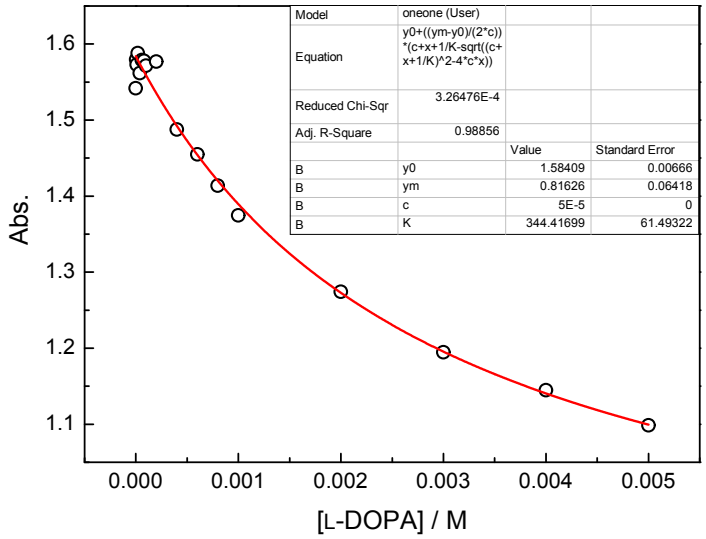

Fig. S18 Curve fit for determination of binding constant of **2** with L-DOPA.

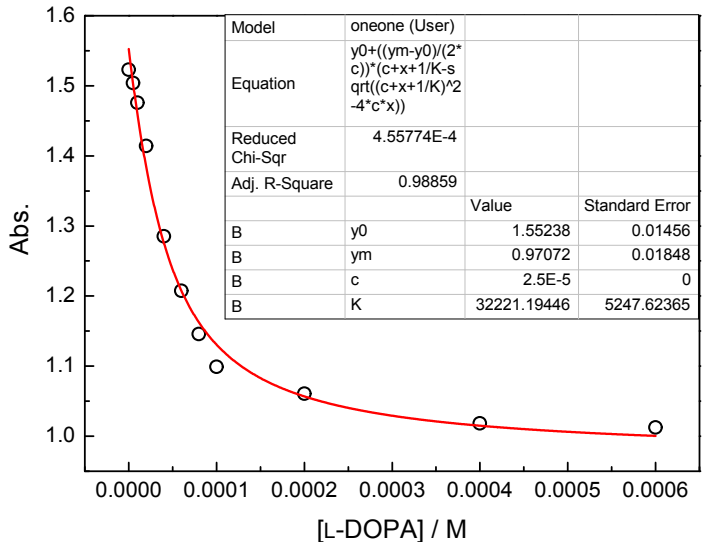

Fig. S19 Curve fit for determination of binding constant of the **1**-**2** ensemble with L-DOPA.

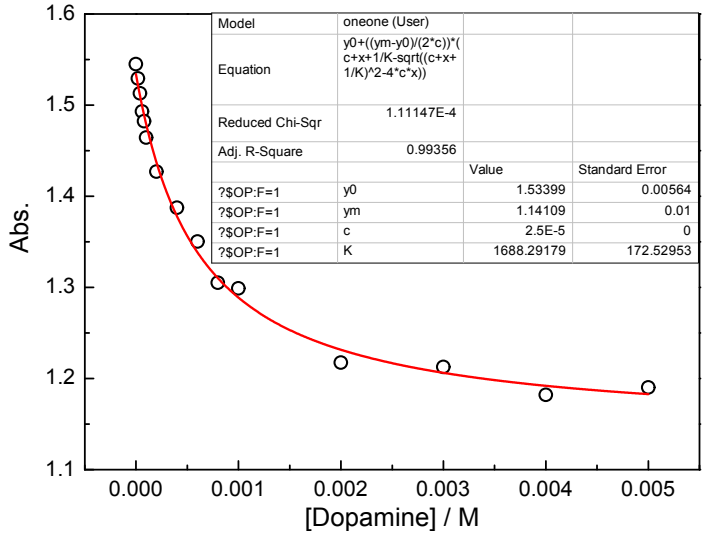

Fig. S20 Curve fit for determination of binding constant of the **1**-**2** ensemble with dopamine.

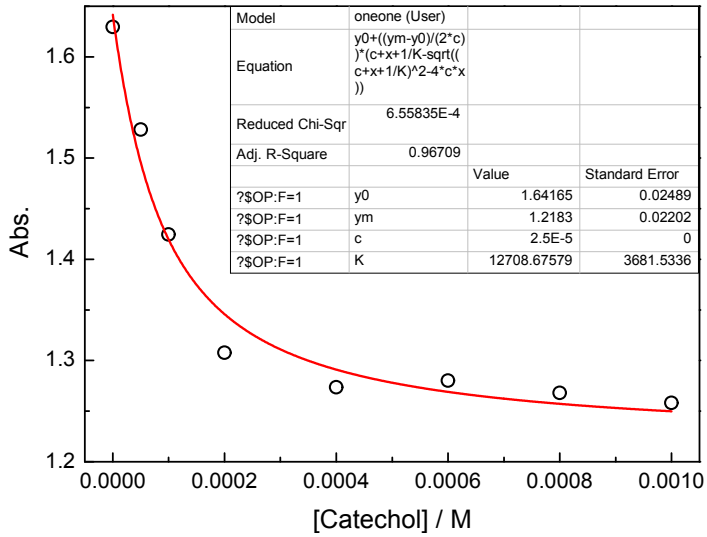

Fig. S21 Curve fit for determination of binding constant of the **1**-**2** ensemble with catechol.

5.1.3 CD spectra and Job plots

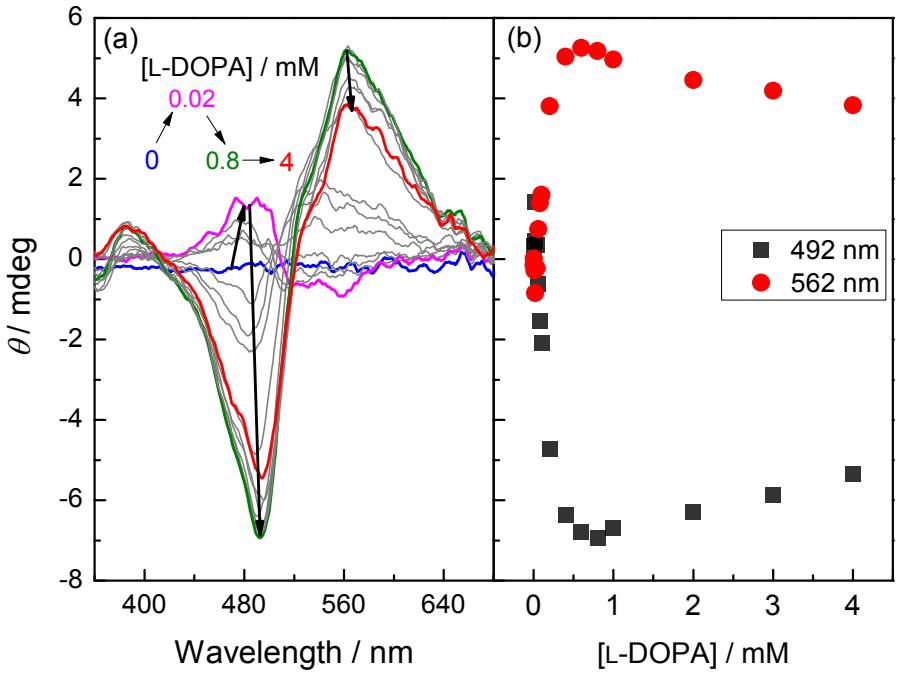

Fig. S22 (a) CD spectra of **1** (50 μM) with increasing concentration of L-DOPA in pH 7.5 HEPES buffer. (b) CD intensity of **1** at 492 nm and 562 nm vs concentration of L-DOPA. Note that with 0.02 mM L-DOPA, the CD spectrum shows negative first and positive second Cotton effects. Upon increasing L-DOPA concentration, the CD spectra show a decrease in intensity, followed by an inversion of the sign. The positive first and negative second Cotton effects reach the maximum intensity at 0.8 mM and decrease upon further increasing L-DOPA concentration. The L-DOPA concentration-dependent aggregate size of **1** shows the same trend (Fig. 3b, black line), with average D_h increasing with increasing L-DOPA concentration till 0.02 mM, followed by a decrease with L-DOPA concentration from 0.02 mM to 0.8 mM, after which the average D_h increases again with further increasing L-DOPA concentration. We propose that different aggregate structures with different L-DOPA to **1** ratios formed throughout the titration. This likely leads to the complexity of UV-Vis absorption titration data (Fig. S11), for which reason the binding constant of **1** with L-DOPA was not calculated.

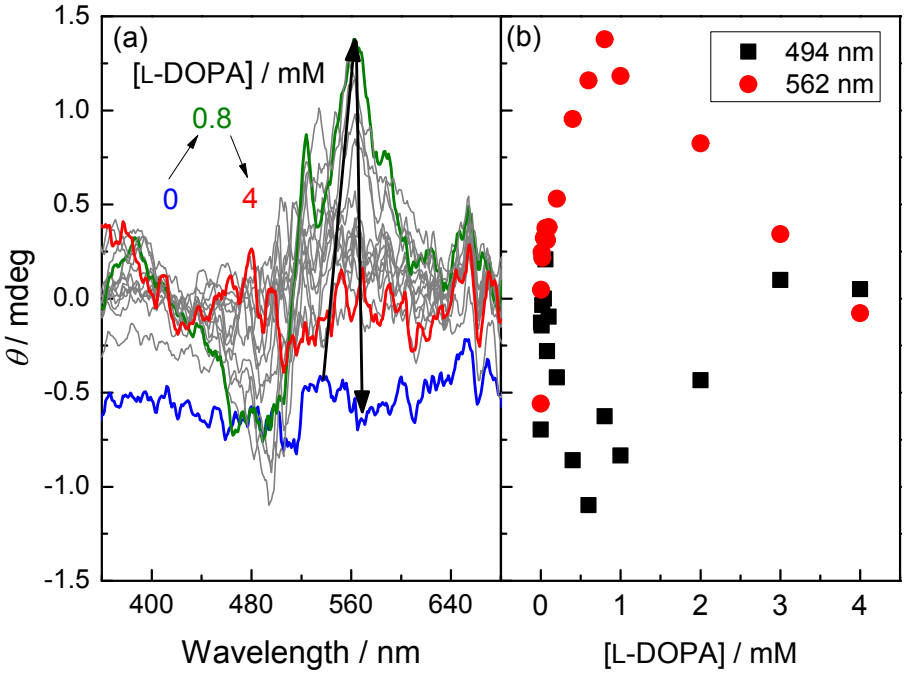

Fig. S23 (a) CD spectra of **2** (50 μM) with increasing concentration of L-DOPA in pH 7.5 HEPES buffer. (b) CD intensity of **2** 494 nm and 562 nm vs concentration of L-DOPA.

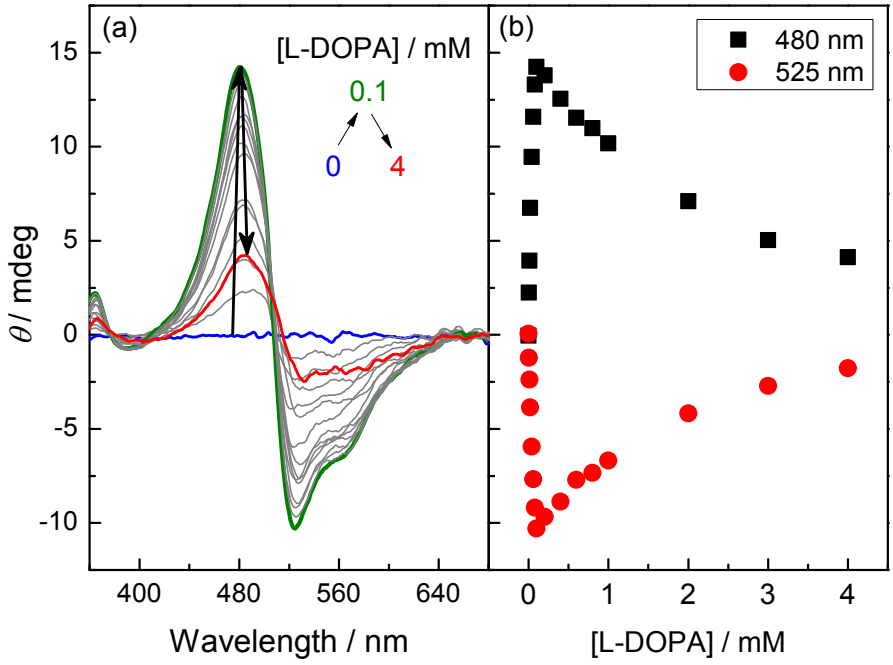

Fig. S24 (a) CD spectra of a mixture of **1** (25 μM) and **2** (25 μM) with increasing concentration of L-DOPA in pH 7.5 HEPES buffer. (b) CD intensity of a mixture of **1** (25 μM) and **2** (25 μM) at 480 nm and 525 nm vs concentration of L-DOPA.

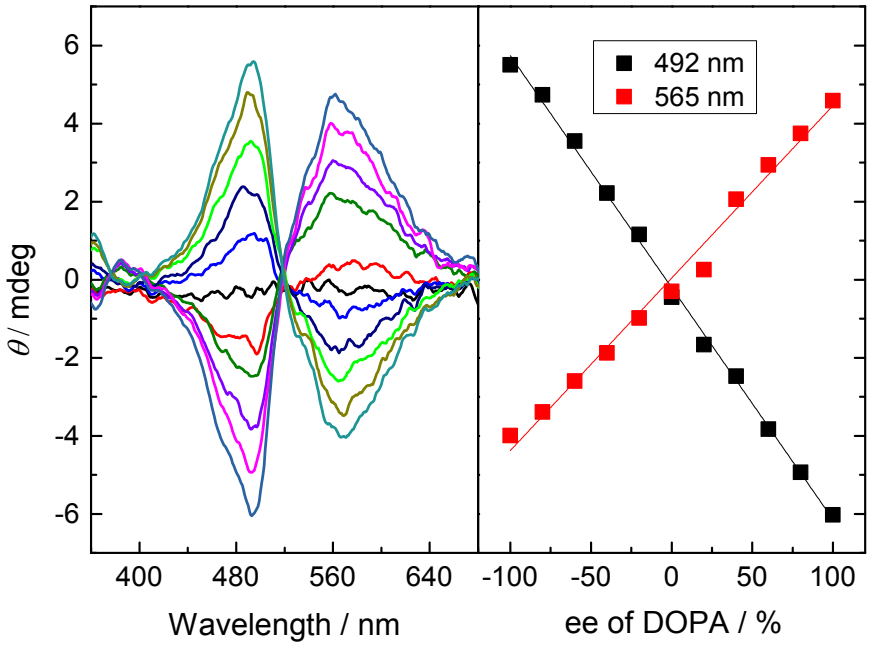

Fig. S25 (a) CD spectra of a mixture of **1** (50 μM) in the presence of DOPA (total concentration 0.8 mM) with different *ee*'s in pH 7.5 HEPES buffer. (b) CD intensity of a mixture of **1** (50 μM) at 492 nm and 565 nm vs *ee* of DOPA.

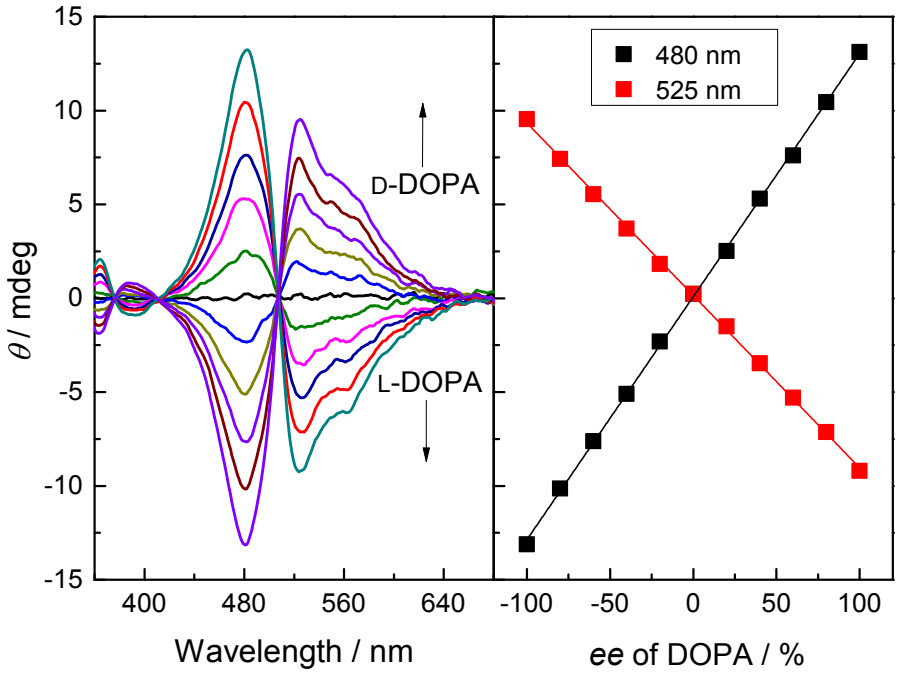

Fig. S26 (a) CD spectra of a mixture of **1** (25 μM) and **2** (25 μM) in the presence of DOPA (total concentration 0.1 mM) with different *ee*'s in pH 7.5 HEPES buffer. (b) CD intensity of a mixture of **1** (25 μM) and **2** (25 μM) at 480 nm and 525 nm vs *ee* of DOPA.

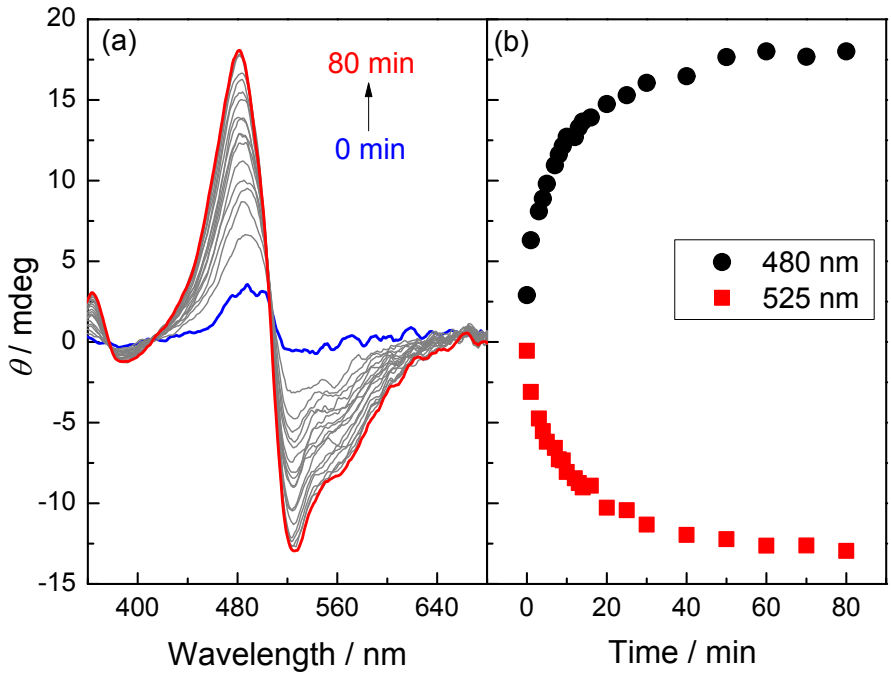

Fig. S27 (a) Time-dependent CD spectra of a mixture of **1** (25 μM) and **2** (25 μM) in the presence of L-DOPA (0.1 mM) in pH 7.5 HEPES buffer. (b) CD intensity of a mixture of **1** (25 μM) and **2** (25 μM) at 480 nm and 525 nm vs time.

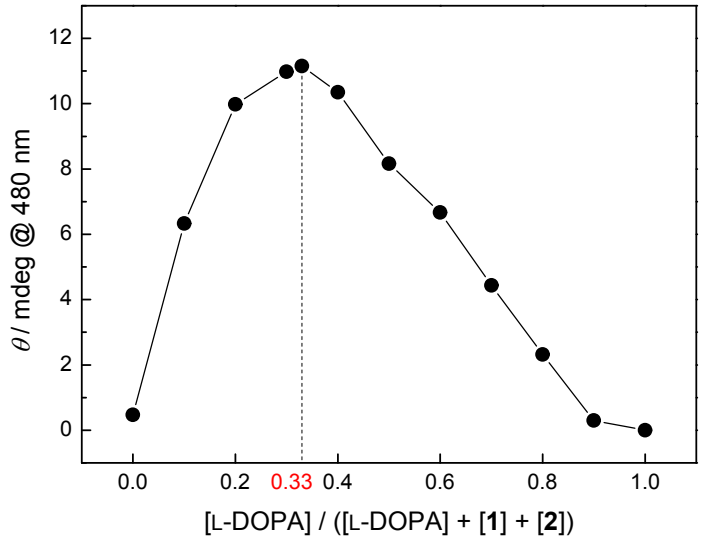

Fig. S28. Job plot analysis for determination of stoichiometry between L-DOPA and the PBI dyes in total, based on the CD intensity at 480 nm. Equal amounts of **1** and **2** were used, and the molar ratio of L-DOPA was varied from 0 to 1, with the total concentration of **1**, **2** and L-DOPA fixed at 0.1 mM.

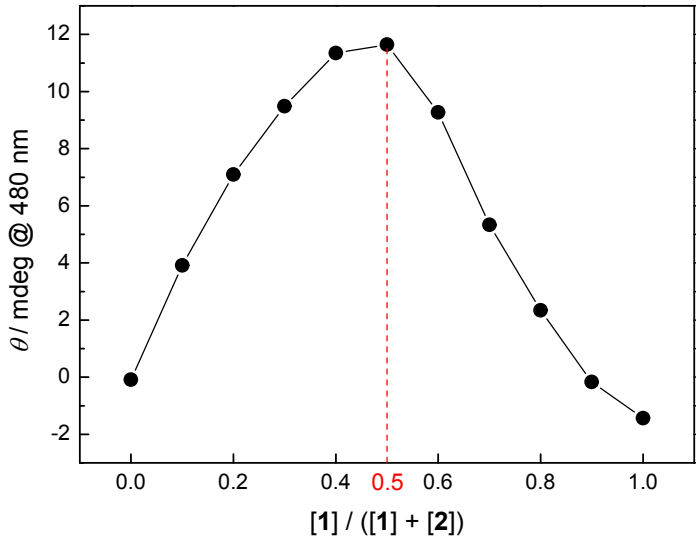

Fig. S29 Job plot analysis for determination of stoichiometry between **1** and **2** based on the CD intensity at 480 nm. The concentration of L-DOPA was fixed at 0.1 mM. The molar ratio of **1** or **2** was varied from 0 to 1, with the total concentration of **1** and **2** fixed at 50 μM.

5.1.4 Selectivity

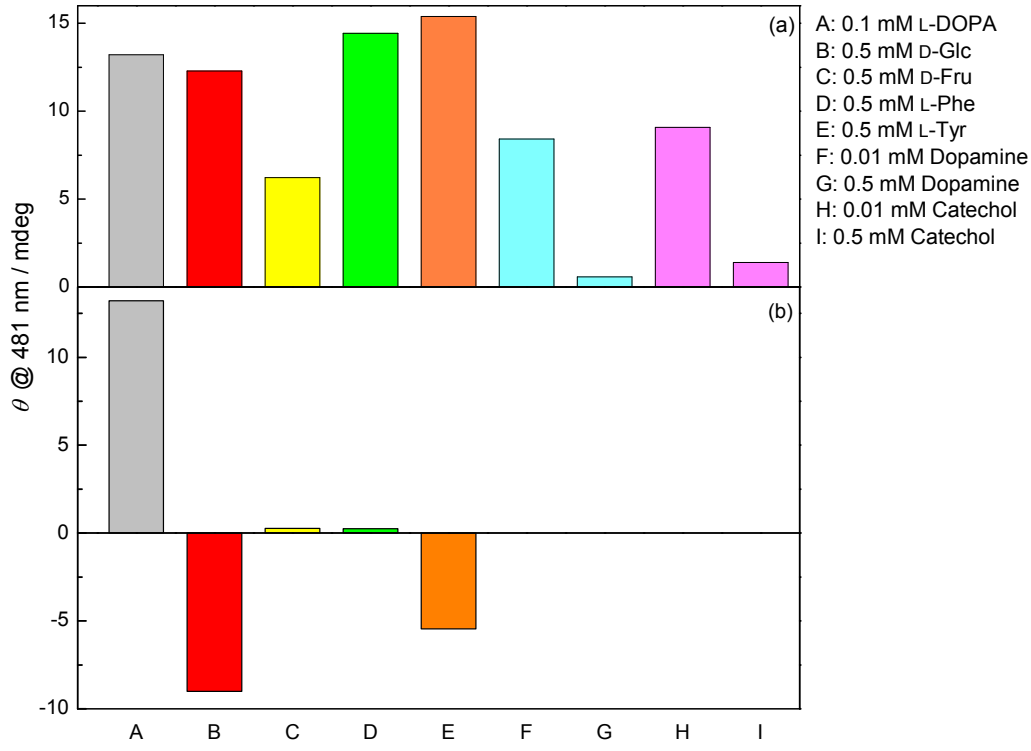

Fig. S30 CD intensity of a mixture of **1** (25 μM) and **2** (25 μM) at 480 nm in the presence of L-DOPA (0.1 mM) coexisting with the indicated substrates (a, B-I) or in the presence of the indicated substrates alone (b, B-I) in pH 7.5 HEPES buffer. The CD response of a mixture of **1** (25 μM) and **2** (25 μM) to L-DOPA (0.1 mM) is shown for comparison (a, A and b, A).

5.2 Compounds 5 and 6 and their mixture

5.2.1 UV-Vis absorption and CD spectra

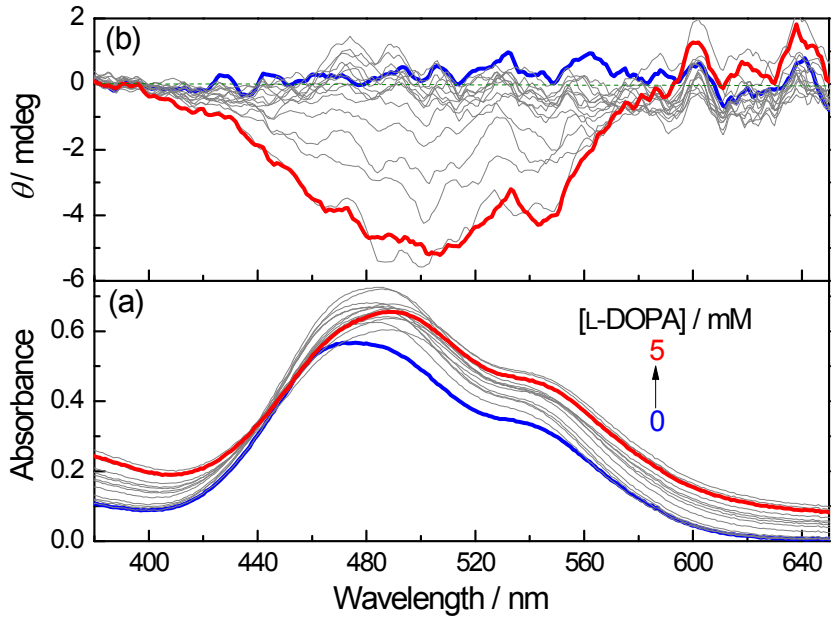

Fig. S31 UV-Vis absorption (a) and CD (b) spectra of **5** (50 μM) with increasing concentration of L-DOPA in pH 7.5 HEPES buffer.

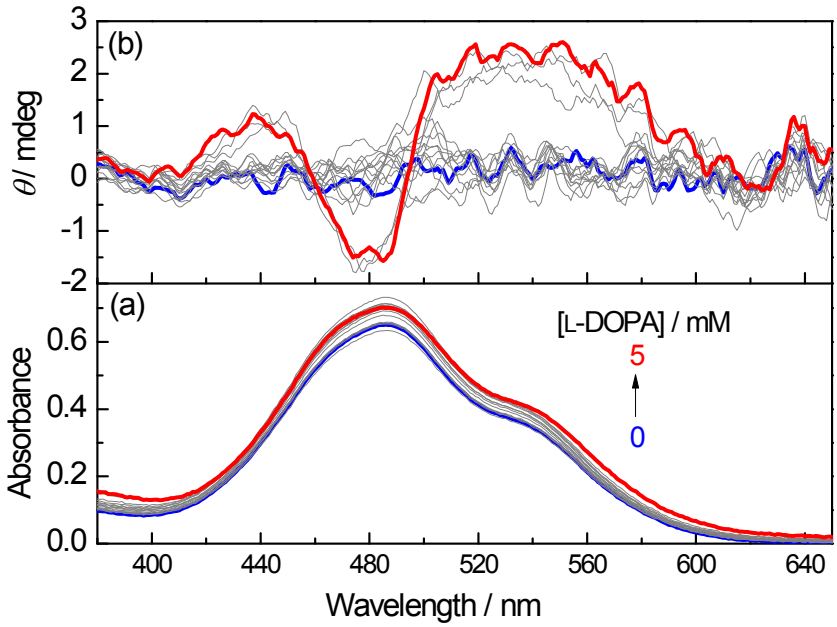

Fig. S32 UV-Vis absorption (a) and CD (b) spectra of **6** (50 μM) with increasing concentration of L-DOPA in pH 7.5 HEPES buffer.

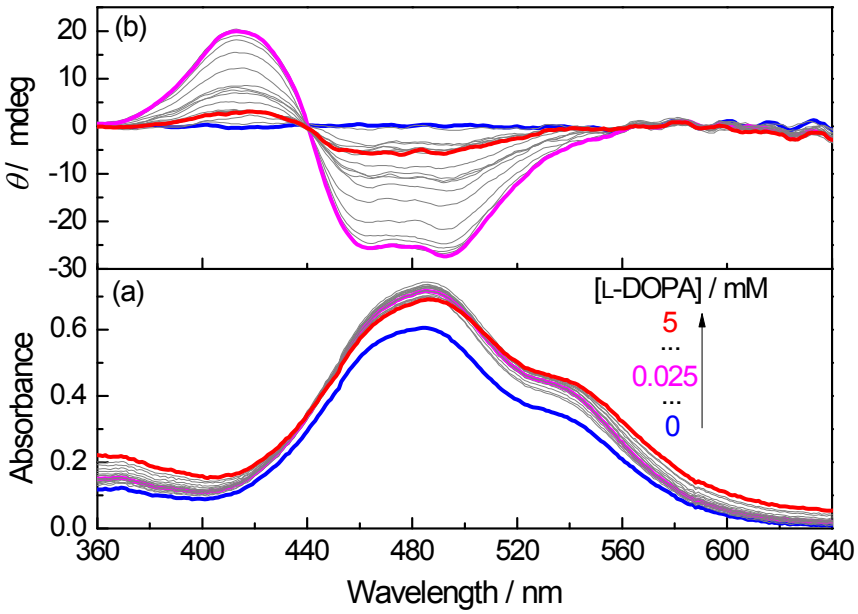

Fig. S33 UV-Vis absorption (a) and CD (b) spectra of a mixture of **5** (25 μM) and **6** (25 μM) with increasing concentration of L-DOPA in pH 7.5 HEPES buffer. The change in the UV-Vis absorption spectra of the perylene chromophore induced by L-DOPA was too small for binding constant determination.

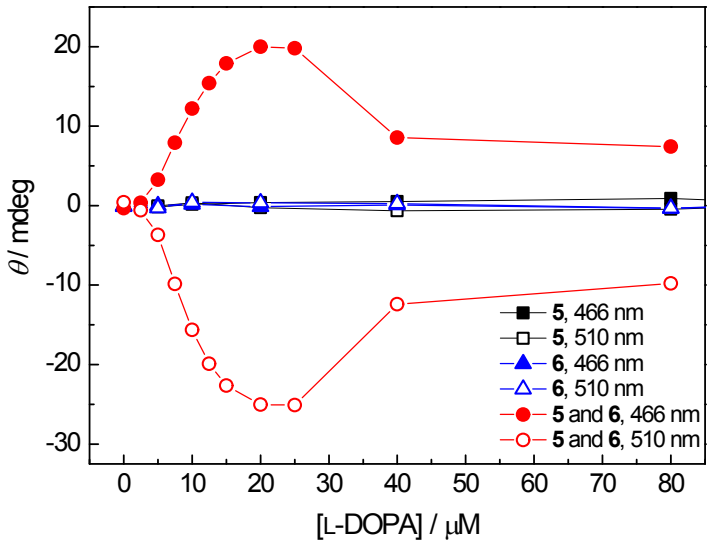

Fig. S34 CD intensity of **1** (50 μM), **2** (50 μM), or a mixture of **1** (25 μM) and **2** (25 μM) at 466 nm and 510 nm vs concentration of L-DOPA.

5.2.2 Job plots

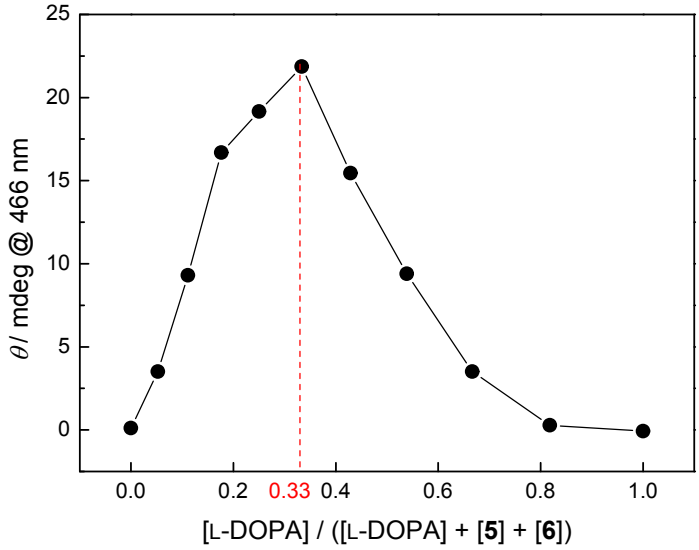

Fig. S35. Job plot analysis for determination of stoichiometry between L-DOPA and the PBI dyes in total, based on the CD intensity at 480 nm. Equal amounts of **5** and **6** were used, and the molar ratio of L-DOPA was varied from 0 to 1, with the total concentration of **5**, **6** and L-DOPA fixed at 50 μM.

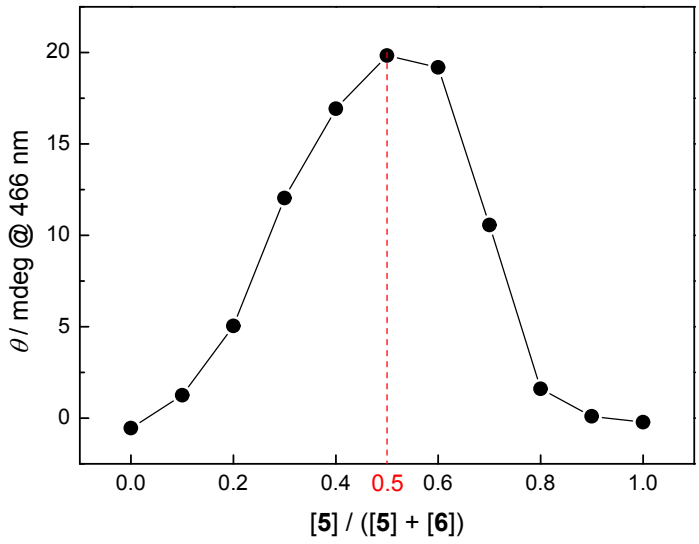

Fig. S36 Job plot analysis for determination of stoichiometry between **5** and **6** based on the CD intensity at 466 nm. The concentration of L-DOPA was fixed at 25 μM. The molar ratio of **5** or **6** was varied from 0 to 1, with the total concentration of **5** and **6** fixed at 50 μM.

5.3 Mixture of compounds 1 and 3

5.3.1 UV-Vis absorption spectra

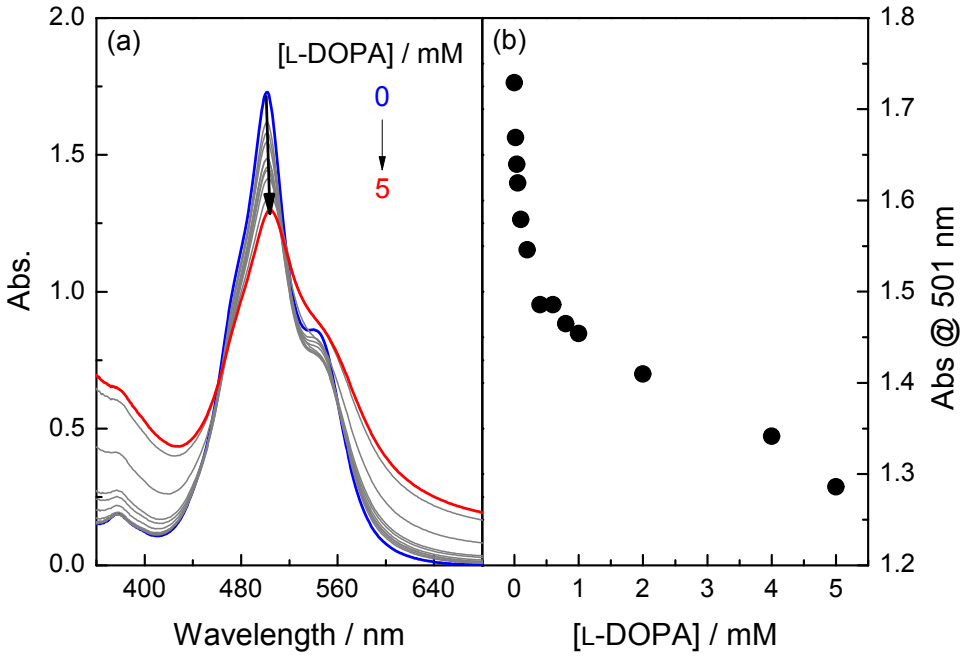

Fig. S37 (a) Absorption spectra of a mixture of **1** (25 μM) and **3** (25 μM) with increasing concentration of L-DOPA in pH 7.5 HEPES buffer. (b) Absorbance of a mixture of **1** and **3** at 501 nm vs concentration of L-DOPA.

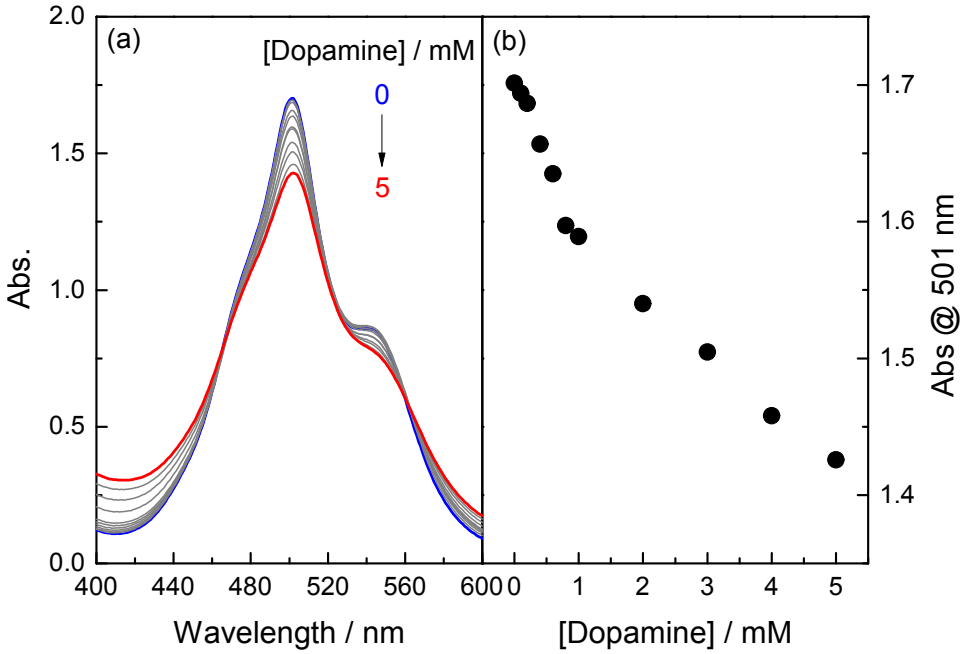

Fig. S38 (a) Absorption spectra of a mixture of **1** (25 μM) and **3** (25 μM) with increasing concentration of dopamine in pH 7.5 HEPES buffer. (b) Absorbance of a mixture of **1** and **3** at 501 nm vs concentration of dopamine.

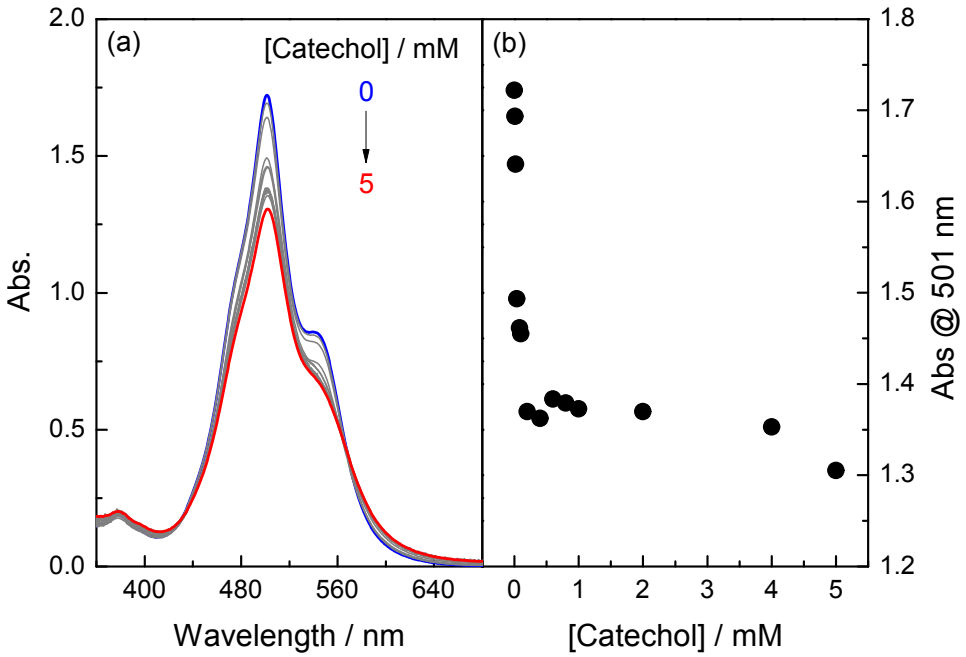

Fig. S39 (a) Absorption spectra of a mixture of **1** (25 μM) and **3** (25 μM) with increasing concentration of catechol in pH 7.5 HEPES buffer. (b) Absorbance of a mixture of **1** and **3** at 501 nm vs concentration of catechol.

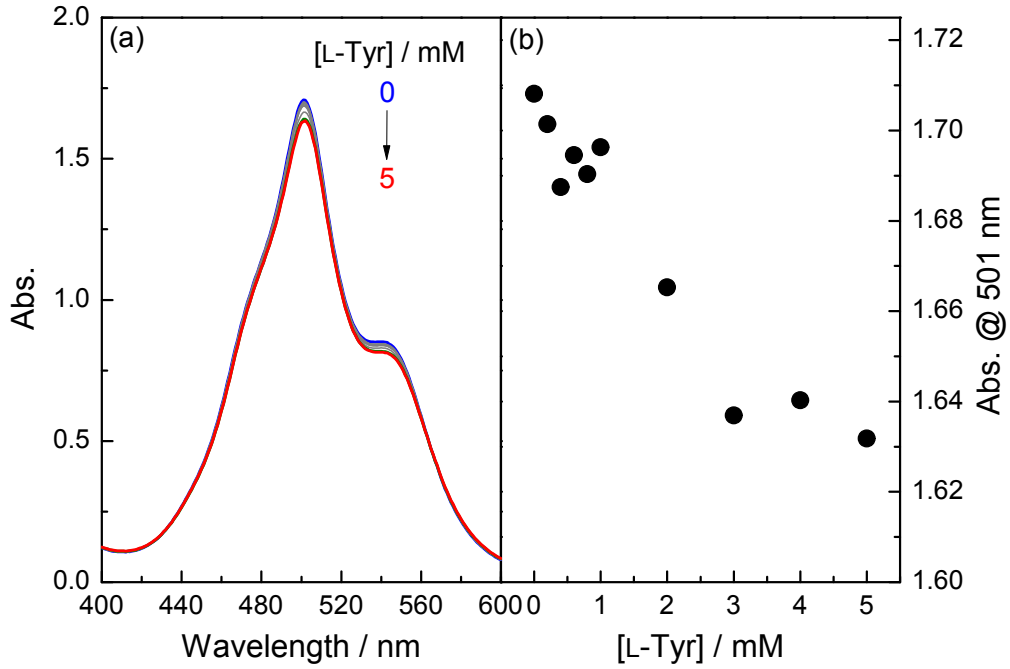

Fig. S40 (a) Absorption spectra of a mixture of **1** (25 μM) and **3** (25 μM) with increasing concentration of L-Tyr in pH 7.5 HEPES buffer. (b) Absorbance of a mixture of **1** and **3** at 501 nm vs concentration of L-Tyr.

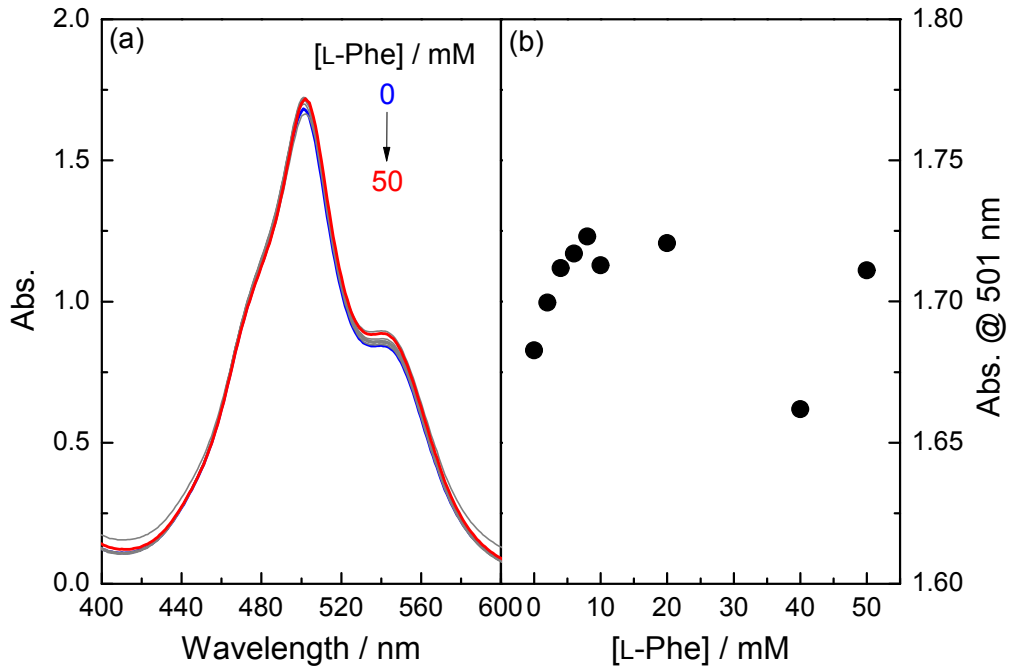

Fig. S41 (a) Absorption spectra of a mixture of **1** (25 μM) and **3** (25 μM) with increasing concentration of L-Phe in pH 7.5 HEPES buffer. (b) Absorbance of a mixture of **1** and **3** at 501 nm vs concentration of L-Phe.

5.3.2 Binding constant determination

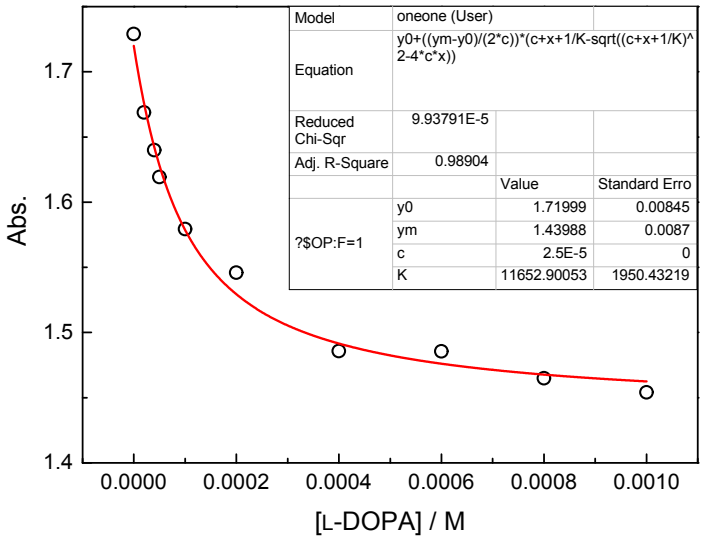

Fig. S42 Curve fit for determination of binding constant of the **1**-**3** ensemble with L-DOPA.

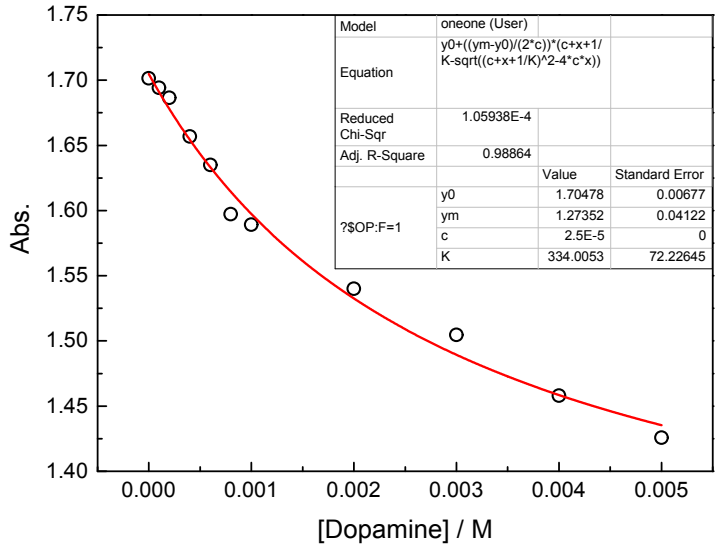

Fig. S43 Curve fit for determination of binding constant of the **1-3** ensemble with dopamine.

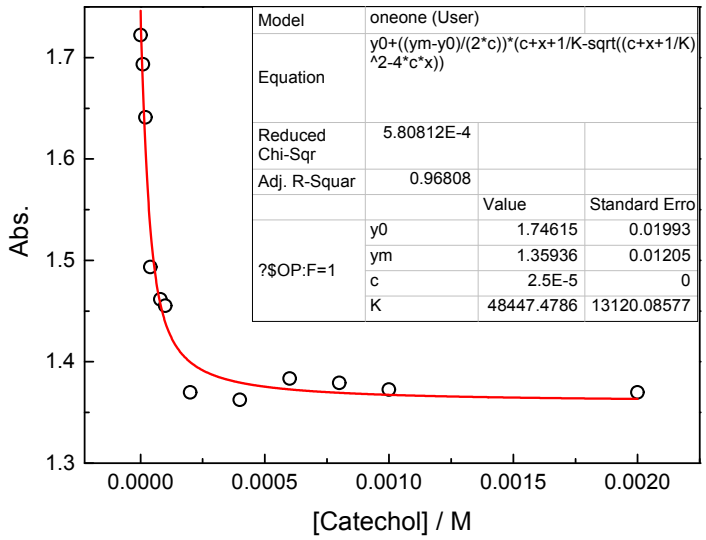

Fig. S44 Curve fit for determination of binding constant of the **1-3** ensemble with catechol.

5.3.4 CD spectra

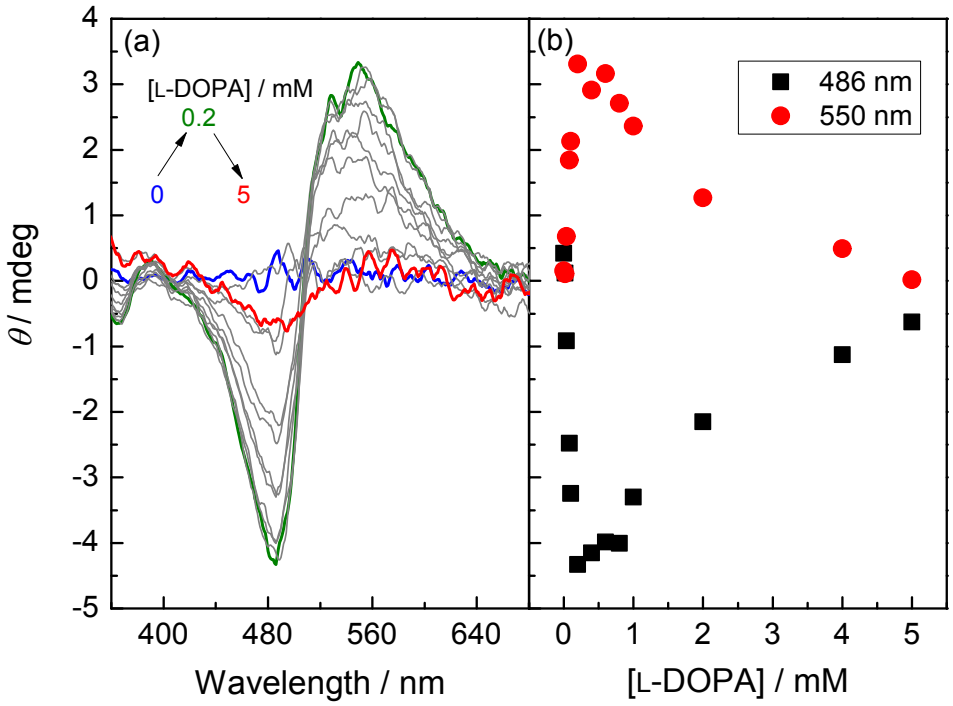

Fig. S45 (a) CD spectra of a mixture of **1** (25 μM) and **3** (25 μM) with increasing concentration of L-DOPA in pH 7.5 HEPES buffer. (b) CD intensity of a mixture of **1** (25 μM) and **3** (25 μM) at 486 nm and 550 nm vs concentration of L-DOPA.

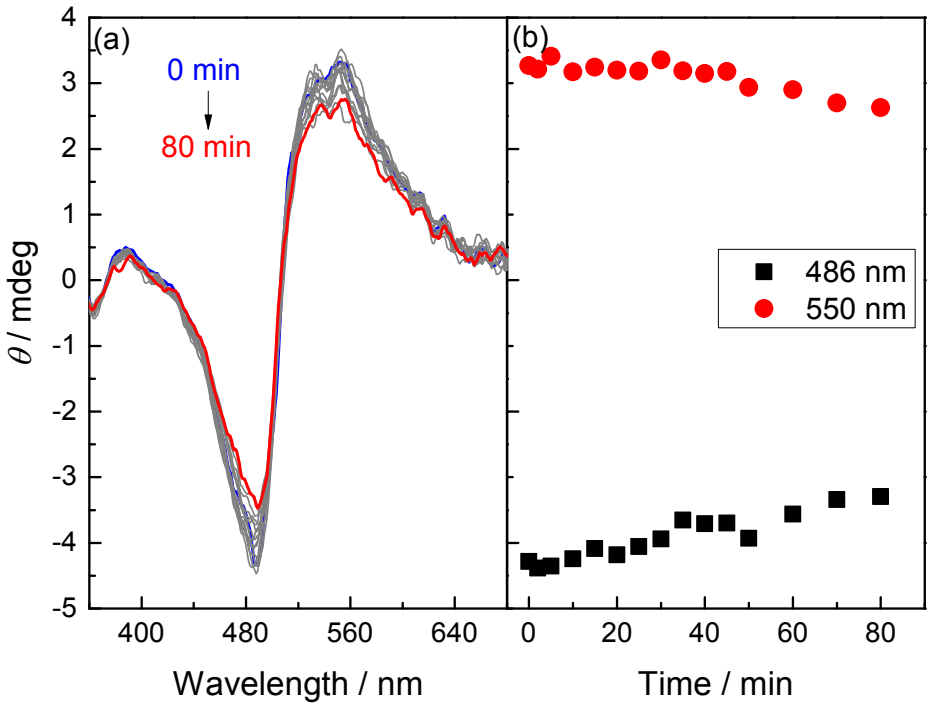

Fig. S46 (a) Time-dependent CD spectra of a mixture of **1** (25 μM) and **3** (25 μM) in the presence of L-DOPA (0.1 mM) in pH 7.5 HEPES buffer. (b) CD intensity of a mixture of **1** (25 μM) and **3** (25 μM) at 486 nm and 550 nm vs time.

5.4 Mixture of compounds 1 and 4

5.4.1 UV-Vis absorption spectra

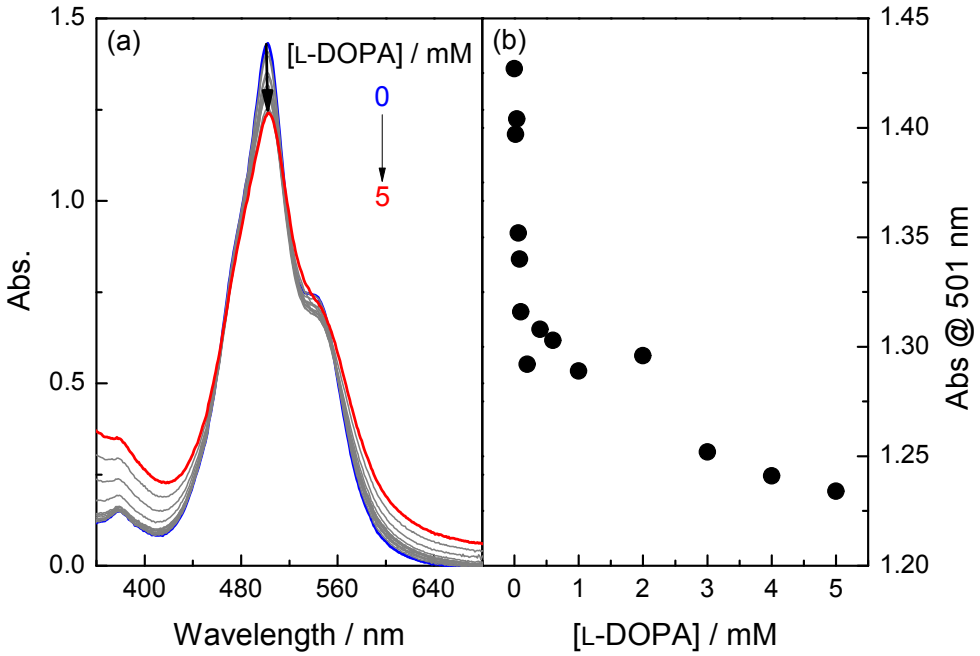

Fig. S47 (a) Absorption spectra of a mixture of **1** (25 μM) and **4** (25 μM) with increasing concentration of L-DOPA in pH 7.5 HEPES buffer. (b) Absorbance of a mixture of **1** and **3** at 501 nm vs concentration of L-DOPA.

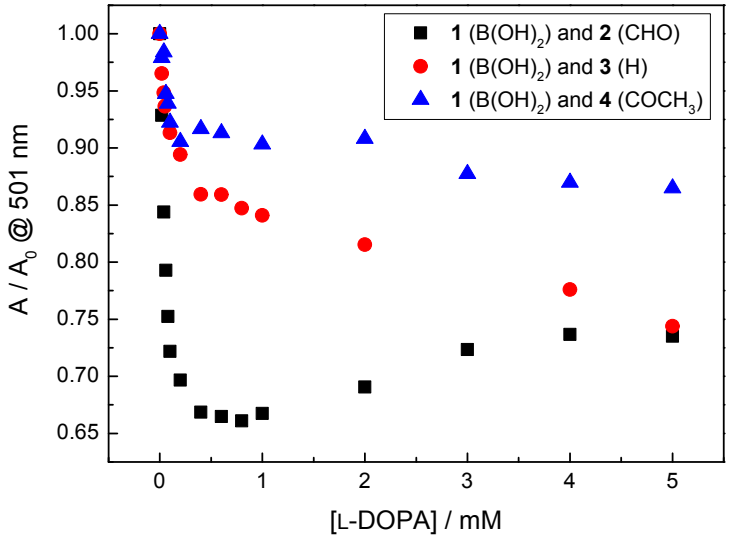

Fig. S48 Comparison of L-DOPA-induced absorption quenching of different dye mixtures. Both **1** and the other dye component were used at 25 μM.

5.4.2 CD spectra

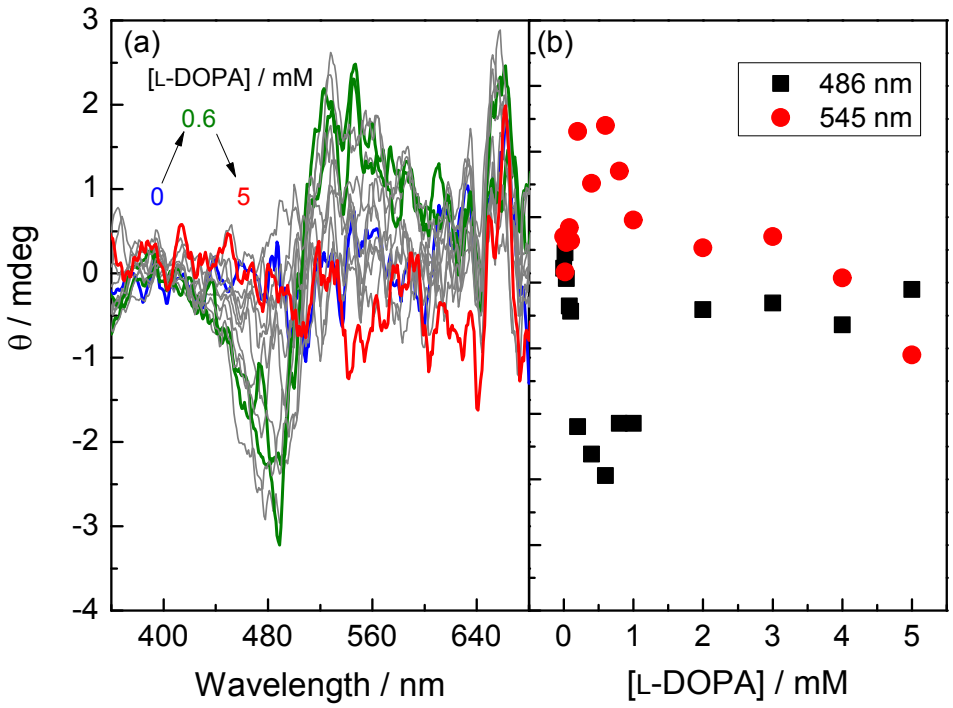

Fig. S49 (a) CD spectra of a mixture of **1** (25 μM) and **4** (25 μM) with increasing concentration of L-DOPA in pH 7.5 HEPES buffer. (b) CD intensity of a mixture of **1** (25 μM) and **4** (25 μM) at 486 nm and 545 nm vs concentration of L-DOPA.

6. References

1. X. Wu, X.-X. Chen, B.-N. Song, Y.-J. Huang, Z. Li, Z. Chen, T. D. James and Y.-B. Jiang, *Chem. Eur. J.*, 2014, **20**, 11793-11799.
2. O. Iliashevsky, L. Amir, R. Glaser, R. S. Marks and N. G. Lemcoff, *J. Mater. Chem.*, 2009, **19**, 6616-6622.
3. R. Wang, Z. Shi, C. Zhang, A. Zhang, J. Chen, W. Guo and Z. Sun, *Dyes. Pigments*, 2013, **98**, 450-458.